Research papers

An IGDT approach for the multi-objective framework of integrated energy hub with renewable energy sources, hybrid energy storage systems, and biomass-to-hydrogen technology

Pham Van Phu [a], Truong Hoang Bao Huy [a], Seongkeun Park [b,*], Daehee Kim [a,*]

[a] *Department of Future Convergence Technology, Soonchunhyang University, Asan-si, Chungcheongnam-do 31538, South Korea*
[b] *Department of Smart Automobile, Soonchunhyang University, Asan-si, Chungcheongnam-do 31538, South Korea*

ARTICLE INFO

ABSTRACT

The decarbonization of electric power systems plays a critical role in global endeavors to mitigate climate change and facilitate the transition towards a sustainable energy future. In this context, green hydrogen has emerged as a promising and nascent clean energy solution, showing substantial potential for addressing the prevailing energy and environmental challenges on a global scale. This paper proposes an integrated energy hub (IEH) operational model to produce green hydrogen from biomass. This model includes renewable photovoltaic and wind sources, biomass electrolyzers, batteries, and hydrogen storage systems (HSS). To effectively manage the uncertainties stemming from renewable sources, electricity and hydrogen demand, and energy prices, an Information Gap Decision Theory-based normalized weighted-sum (IGDT-NWS) approach is proposed. For the first time, this approach solves multi-objective problems with operation costs, carbon emissions, and the energy export index while accounting for uncertainties to mitigate adverse impacts. The planning obtained for IEH with a risk-averse strategy, where the critical deviation factor is 0.1, is robust against the maximum prediction error of electricity demand, hydrogen demand, the output of PV and WT, and the electricity price of 5 %, 1.24 %, 10 %, 7.06 %, and 17.2 %, respectively. With a risk-seeker strategy, our proposed method can optimistically reduce operation cost by 10 % with the deviation of 4.83 %, 5.86 %, 10 %, 0 %, and 5 %, respectively. Moreover, this study emphasizes the potential benefits of integrating HSS into the battery energy storage system (BESS). The results show that the proposed model decreases IEH operation cost by 35.29 %, reduces environmental impact by 33.37 %, and improves EEI by 71.6 %, compared with using BESS only.

1. Introduction

1.1. Background

Currently, countries worldwide strive to achieve ambitious climate targets and transition to sustainable and low-carbon systems, prioritizing decarbonizing the energy sector [1]. A multigeneration system called an integrated energy hub (IEH) allows for the production, transmission, storage, and consumption of various energy carriers to satisfy various requirements [2,3]. The IEH demonstrates its environmental friendliness by frequently harnessing renewable energy sources to fulfill energy requirements, thereby contributing to sustainability in energy generation. Using energy storage systems for efficient energy supply management can help balance energy production and demand. In

addition, energy storage systems can facilitate the utilization of renewable energy sources and increase the flexibility of energy hubs [4–6]. Alternatively, the surplus energy can be transformed into alternative forms, for instance, through electrolysis, to produce hydrogen, which can subsequently be traded in the hydrogen market (HM) to enhance profit. Hydrogen is a promising source of clean fuel and industrial feedstock. The prevailing global method of H2 production relies heavily on fossil fuel sources such as natural gas, coal, and crude oil [7]. This approach significantly increases carbon dioxide emissions, escalating atmospheric greenhouse gases and aggravating global warming. Increasing decarbonized green hydrogen, produced by electrolysis using renewable resources, can significantly reduce industrial production processes and electricity generation emissions. Electrolysis of biomass, a rising and potential technology, can produce hydrogen by replacing the energy-demanding oxygen (O2) production process in water electrolysis

* Corresponding authors.
E-mail addresses: keiny@sch.ac.kr (S. Park), daeheekim@sch.ac.kr (D. Kim).

Nomenclature

Abbreviations

AEL	alkaline electrolysis
BCS	battery charging stations
BESS	battery energy storage system
CHP	combined heat and power
DFB	dual fluidized bed
EEI	energy export index
EH	energy hub
G2I	grid-to-IEH
H2	hydrogen
HM	hydrogen market
HSS	hydrogen storage system
I2G	IEH-to-grid
IEH	integrated energy hub
IGDT-NWS	Information Gap Decision Theory-based normalized weighted-sum
LEC	local energy community
MILP	mixed-integer linear programming
NWS	normalized weighted-sum approach
O2	oxygen
OECD	Organisation for Economic Co-operation and Development
OER	oxygen evolution reaction
P2X	power-to-X
PEM	proton exchange membrane
POM	polyoxometalate
PV	photovoltaic
RES	renewable energy source
SMR	steam methane reforming
SOC	state of charge
SOE	state of energy
WT	wind turbine

Parameters and variables

A_c	surface area of the electrode
a_1/a_2	parameters associated with the ohmic resistance
DOD^{BESS}	BESS depth of discharge
F	Faraday constant
H_t^{demand}	hydrogen demand at time t
H_t^{HSS}	H2 storage volume at interval t (kg)
$\overline{H}^{HSS}$	lower and upper capacity limits of HSS
I_t^c	electrolysis current at interval t (A)
M_{H_2}	molar mass of H2
m_t^{elz}, m_t^{HSS}	hydrogen production rate, output of HSS at interval t (kg)
N_c	the number of series cells
P_t^{elz}	power consumptions of electrolyzer stack at interval t
P_t^{G2I}	power purchased from the grid at interval t (kW)
P_t^{I2G}	power sold back to the grid at interval t (kW)
$\overline{P}^{G2I}$	maximum power can be purchased from grid
$\overline{P}^{I2G}$	maximum power can sold to grid
P_t^{PV}, P_t^{WT}	outputs of PV and WT at interval t (kW)
$P^{BESS,ch}$	BESS charging power at interval t (kW)
$P^{BESS,dis}$	BESS discharging power (kW)
$\overline{P}^{BESS,ch}, \overline{P}^{BESS,dis}$	BESS charging/discharging rate (kW)
Q_{H_2}	heating value of hydrogen (kWh/kg)
T	number of time slots
u_t^c, u_t^{elz}	electrolyzer cell voltage, electrolytic stack voltage at interval t (V)
u_t^{G2I}	binary variable – 1 if IEH purchases power from grid; otherwise 0
u_t^{I2G}	binary variable – 1 if IEH sells power to grid; otherwise 0
$u^{BESS,ch}$	binary variable – 1 if BESS is charging; otherwise 0
$u^{BESS,dis}$	binary variable – 1 if BESS is discharging; otherwise 0
$v_{rated}, v_{cut\,in}, v_{cut\,out}$	rated wind speed, cut in and cut out wind speeds (m/s)
ΔG_{bio}	free Gibbs energy of the biomass electrolysis
$\Delta\tau$	time step (hour)
ε_t^{BESS}	BESS state of energy at interval t
$\overline{\varepsilon}^{BESS}$	maximum SOE of the BESS
ε_t^{HSS}	HSS state of energy at interval t
$\underline{\varepsilon}^{HSS}, \overline{\varepsilon}^{HSS}$	minimum and maximum SOE of the HSS
$\widetilde{\lambda}_t$	forecast data at interval t
η^{elz}	electrolysis efficiency
η^{PV}	conversion efficiency of the solar PV system
η^{BESS}	BESS charge/discharge efficiency
v_t	solar irradiance at time interval t

with the thermodynamically advantageous oxidation of biomass. This replacement significantly reduces electrical consumption, rendering biomass electrolysis an increasingly energy-efficient substitute for traditional power-to-gas (P2G) methods [8]. Achieving sustainable cities requires strategically utilizing renewable energy sources, effectively converting waste into energy, reducing emissions, and enhancing reliability. IEHs play a crucial role in this endeavor by integrating renewable sources, such as solar, wind, and biomass, to meet consumer energy demands. Consequently, ensuring the optimal operation of these renewable-integrated energy hubs is crucial for driving sustainable urban development.

1.2. Literature review

Currently, more than 98 % of hydrogen (H2) production originates from nonrenewable resources [9]. The primary methods employed are natural gas steam methane reforming (SMR), which is responsible for 76 % of worldwide production, and coal gasification, which contributes 22 %. Hydrogen production by water electrolysis is a mature technology [10,11], and its efficiency exceeds 70 % [12]. Alkaline electrolysis (AEL) technology has been used for over a hundred years, making it the most established technology [13]. It is also the most cost-effective option with

the lowest initial investment and maintenance costs. However, AEL has a limited load range of approximately 20–25 % owing to the potential danger of an explosive mixture that may occur from cross-contamination of the gas streams produced. Zeb et al. proposed a novel concept for electrocatalytic water splitting involving hydrogen production through hydrogen evolution and polyoxometalates (POMs) [14]. Renewable energy sources can be used to decompose water molecules into hydrogen and oxygen through electrolysis. The produced hydrogen can then be transported to various locations using pipelines, trucks, or ships [15]. Additionally, it has the potential for sale in the HM. Hydrogen shows excellent potential as a flexible and emission-free energy option and contributes considerably to a sustainable and eco-friendly future. Green H2 generation via biomass electrolysis is a promising and efficient alternative [16]. Oh et al. [17] used phosphomolybdic acid as a catalyst for the oxidative depolymerization of biomass and an electron mediator redox couple of $Fe3+/Fe2+$ at a much lower potential. This method enables cost-effective hydrogen production with near-perfect faradaic efficiency at low pH levels. Additionally, it offers economic advantages through product generation. Yao et al. studied CO2-neutral H2 production processes through dual fluidized bed (DFB) biomass steam gasification. Their simulation results indicated that the DFB biomass steam gasification process had a high H2 conversion rate (51.4 %) [18].

Production of H2 via biomass electrolysis offers several advantages over water electrolysis. This electrochemical process employs a biomass oxidation reaction instead of the oxygen evolution reaction (OER) used in water electrolysis, thereby reducing the oxidation overpotential and electricity consumption [1]. As RESs continue to be installed in energy systems, there is a need to curtail excess power generation to maintain system reliability. The IEHs can utilize this redundant energy to power biomass electrolysis for H2 production, reduce electricity purchase costs, and maximize the use of underutilized RESs. Thus far, limited research has been conducted on incorporating green hydrogen production from biomass as a substitute for natural gas-based hydrogen production in IEH.

In recent years, an increasing number of related research studies have been conducted owing to the crucial role of IEH development [20]. In [2], an IEH that utilized natural gas to produce electricity and heat to reduce operational costs was optimized. Depreciation has been considered for the components of the IEH during scheduling time, such as combined heat and power (CHP) units, heat generation units, and power generation units. Alizad et al. [21] investigated the economic and technical feasibility of designing P2G-IEH systems under future market conditions. The proposed planning method for the P2G-EH system is a stochastic dynamic planning method that considers the reliability constraints and models the system uncertainty parameters using a scenario-based stochastic method. An operational strategy for an off-grid hybrid hydrogen/electricity refueling station was proposed [22] to maximize profits from supplying electricity/hydrogen to battery electric vehicles and hydrogen fuel cell vehicles. Sorrenti et al. [23] studied how the ratio of renewable energy sources to electrolyzers used to produce hydrogen in a P2X system connected to a grid can impact the P2X economy and carbon emissions. Wenkai Dong et al. proposed a planning model for an IEH with a power grid, gas network, and energy hubs [24]. The goal is to minimize the operational fuel and investment costs through carbon capture and bidirectional energy exchange. Their planning model, which did not consider bidirectional energy exchange, resulted in a 13.47 % annual cost savings compared with the baseline scenario. Luo et al. [25] discussed the optimal scheduling of a district energy system with multiple energy supply modes and flexible loads. The IEH model included an energy storage system and an integrated electric vehicle. This study proposes an optimal scheduling strategy to minimize the multi-energy purchase and emission tax costs. In [26], the IEH model analyzed energy level matching and balance between sources and loads to increase economic efficiency. The two-level planning model optimizes the system structure and component sizing, whereas the lower-level model identifies the optimal operation strategy. A global sensitivity analysis was used to evaluate the uncertainties. A Beijing case study is used to illustrate the methodology. Luo et al. [27] used a hierarchical Stackelberg game to schedule the energy in a three-tier IEH. This hub includes electricity and natural gas firms, smart energy hubs, and users. Multi-time scale coordinated optimization is proposed, which uses multi-energy flows and multi-type energy storage systems to optimize scheduling plans for variable energy resources and load demands [28]. It includes day-ahead economic dispatch, local intraday receding-horizon optimization, and real-time adjustment to minimize the daily operation costs of the IEH. Liu et al. [29] proposed a zoning planning method based on the energy hub model and a directed acyclic graph that can solve regional IEH planning problems without a fixed system structure. This method jointly plans the system structure and equipment configuration, improves computational efficiency, and reduces the total annual cost. Chamandoust et al. developed a method to optimize intelligent IEH system scheduling for cost and emission reduction while maintaining the energy supply probability and optimal load levels [30]. They used demand-side management to shift loads and Monte Carlo modeling for renewable energy sources and loads. Miao et al. [31] proposed IEH model uses renewable sources such as wind and solar power for cooling, heating, and electricity. It manages energy flow, uses storage devices, and aims to reduce costs and CO2 emissions. Yiyang

Qiao proposed a solution to the problems of low efficiency and energy waste caused by neglecting the impact of the energy equipment type and configuration [32]. The solution is a multi-objective optimization method based on the IEH, which focuses on the configuration of gas turbines. The method establishes a multi-objective optimization model that determines the equipment installation configuration and operation strategy while considering the economic, energy consumption, and environmental benefits. Kuan Zhang et al. developed a model for a multi-energy trading framework for a hybrid-renewable-to-H2 provider (HP) capable of converting hybrid renewable energy sources into hydrogen (H2) and trading both H2 and electricity [33]. This framework aims to efficiently utilize renewable energy resources (RESs) while enabling HP to profit from both markets. By utilizing biomass electrolysis and electrochemical effects, the HP can produce green H2 from hybrid RESs and benefit from the flexibility of the electricity-H2 conversion. In general, IEH optimization aims to reduce costs and emissions. Research on balanced solutions that consider economic, technical, and environmental aspects is limited. Some studies have tackled IEH with multiple objectives but have yet to consider the bidirectional energy exchangeability of IEH and uncertainty factors.

In some studies, uncertainty parameters have been used to solve the power and energy systems. Orozco et al. developed a scheduling strategy with a single objective for a local energy community (LEC) based on the alternating direction of multipliers [34]. The authors included intraday operation coordination with day-ahead decisions and a scenario-based approach to account for uncertainties in renewable sources. Zhang et al. [35] proposed a model for managing grid-connected flexible energy hubs, which include electrical and heating networks. The goal is to minimize operating costs while considering demand, energy prices, and renewable power uncertainties by using the transformation method. In [36], a scheduling model was developed for prosumers in the energy community. This model uses a stochastic-robust approach to handle uncertainties arising from energy transactions with a utility grid, community, or peers. Different uncertainty models address the heterogeneity of these unknown parameters to improve economic efficiency. Robust formulations were used for predictable parameters, whereas scenarios were used for highly volatile uncertainties. Norouzi et al. [37] proposed the flexible power management model to minimize the difference between the expected energy cost and the expected profit for a networked microgrid (MG) with renewable energy sources (RESs) and flexibility sources. Stochastic programming is used to model uncertain parameters. Arsalan Najafi et al. presented a hybrid stochastic-robust approach for optimizing short-term hydrogen-based EH by efficiently managing energy procurement to meet demands [38]. Stochastic programming handles demand uncertainties, whereas robust optimization addresses regulatory market price uncertainty. In [39], a new bi-level multi-objective model was developed to optimize microgrid flexibility. Demand, energy price, maximum active renewable generation, and the electric vehicles (EVs) parameters are modeled using hybrid stochastic-robust optimization. Pirouzi proposed an optimal energy management model in a virtual power plant (VPP) [40]. Uncertainty in the system and VPP loads, day-ahead market prices, and wind farm power generation are considered by using hybrid stochastic-robust scheduling. Stochastic methods that are based on risk offer advantages over deterministic methods and scenario-based optimization approaches by considering uncertain variables and providing more comprehensive results. Information Gap Decision Theory (IGDT), an alternative method, can overcome the limitations and shortcomings of other methods because prior knowledge of uncertain parameters is not required. Tostado-Véliz et al. [41] proposed a single-objective optimization model using IGDT to create a scheduling program that considers uncertainty to reduce the adverse effects of uncertain variables, such as renewable energy output, demand, and energy prices. A newly proposed model to improve unit commitment in EHs with electric, thermal, and cooling demands was developed in [42]. The model integrates different storage systems, combined heat and power (CHP) units, boilers, electric chillers,

Table 1
Summary of the reviewed references and the current study in terms of IEH optimization.

Ref	Objective function		Biomass	HSS	Uncertainties				Method
	Single	Multi			RES	Load demand	Energy price	Hydrogen demand	
[2]	✓			✓	✓	✓	✓		Stochastic
[22]	✓			✓					
[23]	✓			✓					
[24]	✓			✓					
[25]	✓								
[26]	✓								
[27]	✓			✓					
[28]	✓			✓					
[29]	✓								
[30,31]		✓							
[32]		✓							
[33]	✓		✓	✓					
[34]	✓				✓	✓			Stochastic
[35]	✓				✓	✓	✓		Unscented transformation
[36]	✓						✓		Hybrid
[38]	✓			✓			✓	✓	Hybrid
[39]		✓			✓	✓	✓		Hybrid
[40]	✓				✓	✓	✓		Hybrid
[41]	✓			✓	✓	✓	✓	✓	IGDT
[42]	✓			✓	✓	✓	✓		IGDT
[43]	✓						✓		IGDT
[44]		✓		✓		✓			IGDT
[45]	✓		✓	✓	✓	✓	✓	✓	IGDT
[46]	✓			✓	✓	✓		✓	Hybrid
[47]		✓			✓	✓			IGDT
[48]		✓			✓	✓			Hybrid
[49]		✓		✓	✓				IGDT
[50]	✓				✓	✓			Hybrid
Present		✓	✓	✓	✓	✓	✓	✓	IGDT

absorption chillers, photovoltaic (PV) modules, wind turbines (WT), and battery charging stations (BCS). The model uses the IGDT to schedule day-ahead EH operations from risk-neutral, risk-averse, and risk-seeking perspectives. The model also considers the uncertainties related to electricity demands, BCS demand, heat demand, cooling demand, PV and wind power outputs, and electricity prices. Tafreshi et al. developed a new model for the optimal operation of an IEH that includes various components such as RESs, plug-in hybrid electric vehicles (PHEVs), fuel cell vehicles, fuel cells, electrolyzers, hydrogen tanks, boilers, inverters, rectifiers, and heat storage systems [43]. This model uses risk-averse and risk-seeking strategies to incorporate the uncertainty associated with the PHEV power consumption during trips. In [44], a new model for generating electrical power was proposed using Reverse Osmosis technology and an Organic Rankine. It includes a parking lot, battery swapping station, electrolyzer, hydrogen tank, and fuel cell to balance the hydrogen production and consumption. The model was evaluated on a commercial building on Qeshm Island using scenario generation and the IGDT method to model existing uncertainties. Nasir et al. [45] focus on scheduling renewable energy sources for the day ahead and is connected to demand response aggregators. The Information Gap Decision Theory (IGDT) is used as a risk-aware method to handle uncertainties related to demand and price. A hybrid approach was created in [46] to address various sources of uncertainty in multi-energy microgrids. This hybrid model uses point estimation methods for renewable energy generation, IGDT for electricity demand, and stochastic programming for hydrogen demand from fuel cell EVs. The MILP model includes both a battery energy storage system (BESS) and a hydrogen storage system (HSS) to provide a comprehensive solution. Wang et al. [47] suggested a scheduling model that considered IEH participation in the carbon market, accounting for uncertainties in renewable energy and load. It introduces a ladder-type carbon-trading mechanism and models risk aversion and preferences based on the IGDT method. This model has both economic and environmental objectives. In [48], the confidence gap decision (CGD) method robustly optimized energy storage by incorporating chance constraints, probability confidence intervals, and

IGDT. It maximizes voltage profile improvement while minimizing investment costs and ensuring safe and efficient energy storage allocation. Mansour-Saatloo et al. [49] propose an optimal energy management strategy for a combined hydrogen, heat, and power microgrid (CHHP-MG) integrated with hydrogen refueling stations and electric vehicle parking lots. It uses a multi-objective Information Gap Decision Theory (IGDT)-based robust approach to handle uncertainties of RES and reduce operation costs. Jokar et al. [50] developed a model for planning a renewable energy system using wind turbines, bio-waste energy units, and stationary and mobile energy storage. Uncertainties in loads, renewable power, and energy consumption of mobile storage devices are addressed using robust optimization based on IGDT. A few studies have considered hydrogen demand uncertainty but only focused on economic improvement.

1.3. Research gaps and motivation

From a literature review perspective, many investigations have been conducted on modeling the IEH for singular and multiple objectives. A concise comparison of the optimization research on the IEH is presented in Table 1. According to this table, the research gap in IEH optimization is identified as follows:

- Owing to the growing impact of climate change, there is an increasing demand for alternative methods of hydrogen production that align with the global trend towards transitioning to an H2-based society. H2 production can be accomplished using thermochemical, biochemical, and electrolytic methods. Methanol steam reforming (MSR) and P2G are widely used for on-site H2 production. However, methanol steam reforming utilizes natural gas as a feedstock to produce CO_2, a greenhouse gas that contributes to climate change. Biomass-hydrogen-based processes are emerging as promising options for increasing the H2 production capacity. Based on electrochemical effects, aqueous electrolysis of native biomass can be powered by wind and solar power to reduce power consumption and
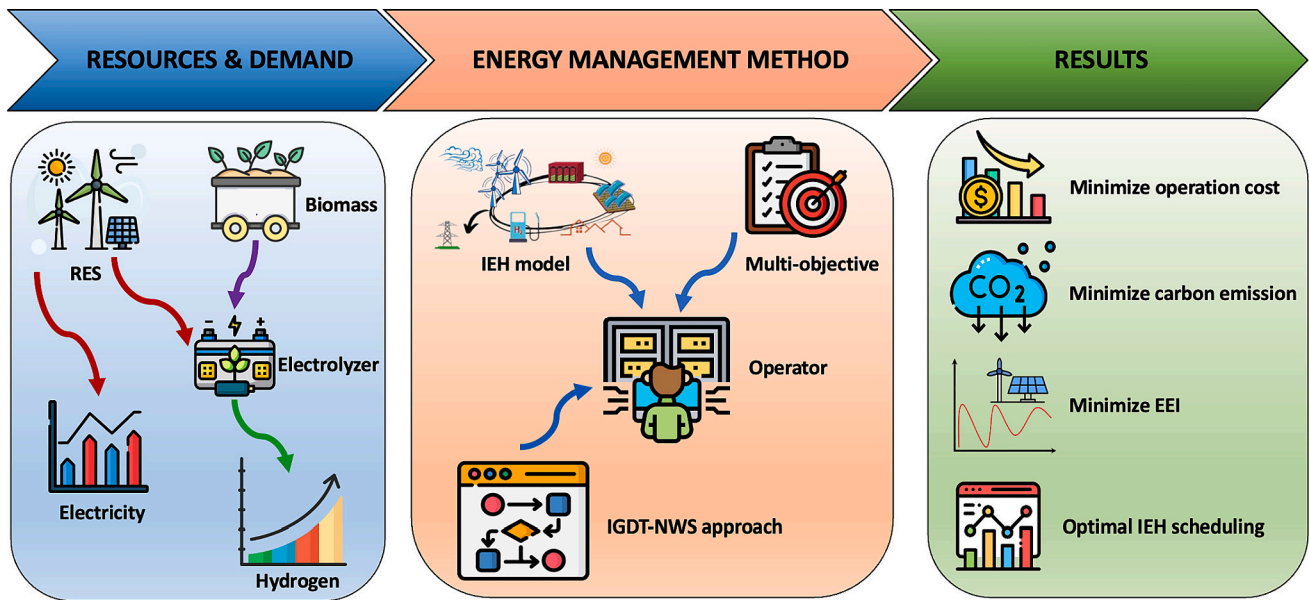
Fig. 1. The overview of the proposed framework.

facilitate on-site hydrogen production. Therefore, integrating green hydrogen production systems from biomass electrolysis as an alternative to natural-gas-based hydrogen production in the IEH optimization problem should be considered.

- Previous research on IEH has primarily viewed them as passive consumers, neglecting their identity as active prosumers and the prospects of energy sales within the market. Although a limited number of studies have presented all-encompassing IEH models, they have solely prioritized the objective of reducing operational costs. Currently, there is an increasing focus on reducing emissions to the environment in order to generate power and improve the power supply capacity of IEHs. A multi-objective paradigm that accounts for the aforementioned factors would render the IEH scheduling problem more comprehensive and realistic.

- The optimization problem of an IEH has been extensively studied in the literature, with two main objectives: operation cost and emission. Given that optimization problems are inherently multi-objective, the IEH problem must be addressed comprehensively, considering all three aspects: economic, technical, and environmental. This approach aims to provide the operator with a solution that balances all the objectives. It is essential to simultaneously account for these objectives to avoid an unbalanced and unrealistic IEH model. Only some studies have addressed the IEH problem with more than two objectives. Still, these studies have defined the IEH as a passive load and an incapacity for bidirectional energy exchange.

- The Integrated Energy Hub (IEH) domain encompasses electricity and other energy forms. The unpredictability of the load can be affected by indoor conditions, building parameters, climate, and social economy, among other factors. Renewable energy output is susceptible to environmental and weather factors. Energy prices are subject to transaction volume errors owing to uncertain factors, such as IEH load, equipment failure, and network transmission capacity. Previous studies have only considered day-ahead data for an IEH model, ignoring the uncertainty of the parameters. Some studies thoroughly considered the above uncertain factors but only solved the single-objective problem. Therefore, a risk-aware approach must be adopted in a multi-objective study to navigate uncertainties and assess their effects on the operational scheduling of IEH.

1.4. Research contributions

Although there have been numerous investigations into hydrogen production in the IEH, significant research gaps still need to be addressed. As listed in Table 1, IEH scheduling is used with different objectives and techniques. However, a holistic model has yet to be proposed for producing green hydrogen from RESs in a reliable way that meets the dynamic demands for electricity and hydrogen throughout the day. The requirement needs an effective technique that models its simultaneous uncertainties while considering the robustness and opportunistic aspects of the uncertain parameters and their occurrence states to generate a more accurate assessment of the system. These gaps in the current research have motivated us to propose a holistic model for the optimal operation of IEH in producing green hydrogen. The main contributions of this study are visually depicted in Fig. 1 and presented as follows:

- An IEH system that uses biomass electrolysis has been proposed to create green hydrogen from renewable sources. This system is designed to be both cost-effective and environmentally friendly by utilizing wind and solar power to power the process. This method dramatically improves the efficiency of the electrolysis process, producing high-quality green hydrogen while reducing electricity consumption. This process also helps break down native biomass and extract electrons, resulting in a more efficient and sustainable production process.

- The optimal operational problem for the IEH considers multiple objectives and uses a formulation that includes three primary functions: financial benefits, reduced carbon emissions, and energy export index. In addition, the problem was designed to analyze the impact of RESs and storage capacity on the IEH by simulating three different expansion cases. These cases include scenarios in which RES, BES, and HSS are unavailable. The impacts of these scenarios were studied in terms of the three primary objective functions mentioned earlier.

- The Information Gap Decision Theory-based normalized weighted-sum (IGDT-NWS) approach is developed to address the multi-objective problem and effectively handle the uncertainties. Specifically, this method utilizes a fractional error model of IGDT to model the uncertainties in predicting renewable energy source output, electricity and hydrogen demand, and energy price. By considering both risk-
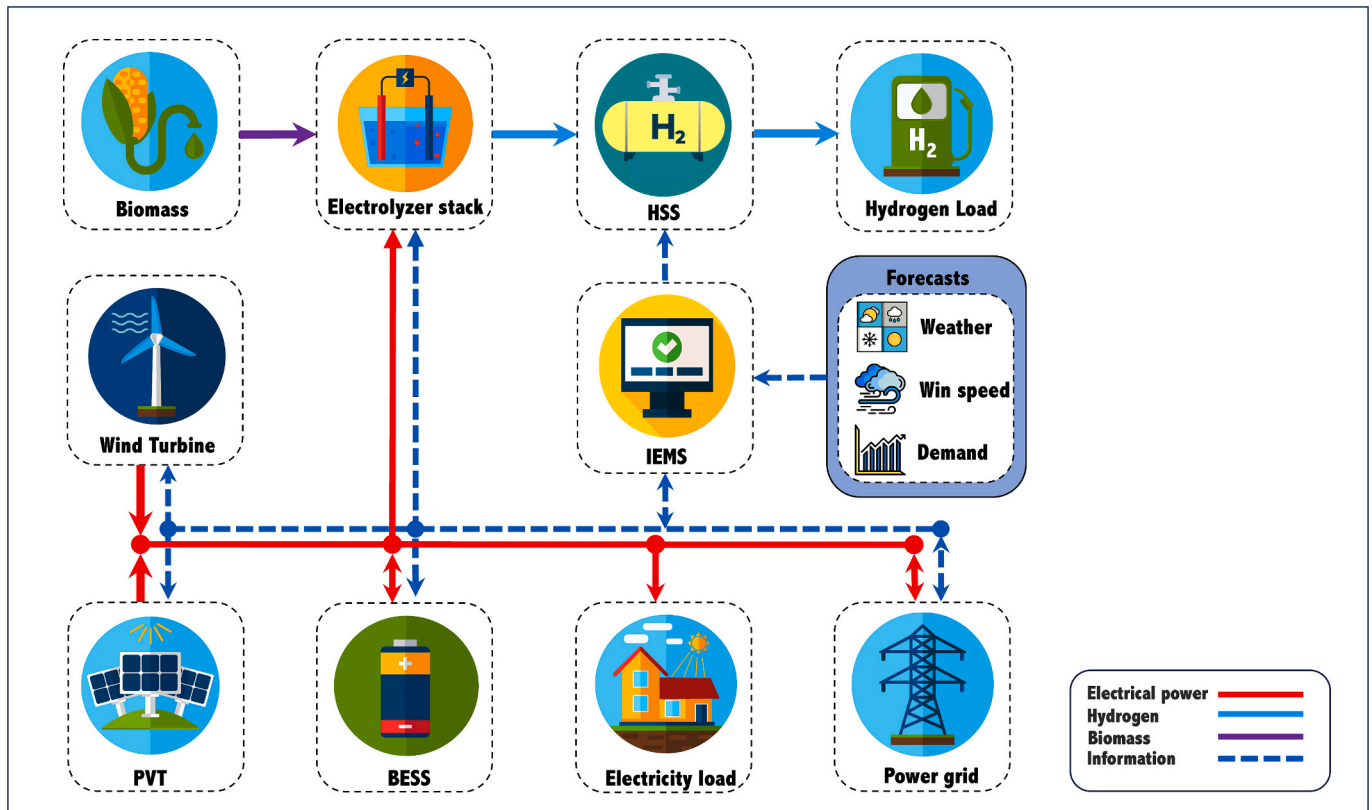
Fig. 2. Schematic of the proposed IEH.

averse and risk-seeking strategies within the IGDT method and various practical scenarios, the proposed model offers a more realistic approach to analyzing the stochastic behavior in the IEH. The normalized weighted-sum approach to solve multi-objective problems resulted in compromised and efficient solutions in which the objectives were close to the ideal values. The IEH operators can consider multiple weighting factor options for each objective to satisfy different operating requirements. The proposed algorithm was compared to a situation that did not consider uncertainties and robust optimization. The comparison results show that considering all factors, the proposed IGDT-NWS method can achieve a better solution.

1.5. Paper layout

Section 2 focuses on problem formulation, while Section 3 describes the proposed IGDT. The simulation results are analyzed in Section 4, and concluding statements are provided in Section 5.

2. Problem formulation

This study aims to develop a comprehensive IEH that uses renewable sources for hydrogen generation through the biomass electrolyzer and stores energy in the BESS and HSS. The IEH can also engage in grid trading and sell hydrogen on the market. Fig. 2 illustrates the typical IEH investigated in this study, which includes the following main components:

- Solar PV systems: This innovative technology harnesses the sun's abundant energy to generate electricity. The system directly converts sunlight into electrical power through the photovoltaic effect by using semiconductor materials in solar panels. This clean and renewable energy source offers a sustainable solution, reducing the reliance on fossil fuels and carbon emissions.

- Wind-turbine power system: This system consists of large blades that rotate when exposed to wind currents and generate mechanical energy. This energy was converted into electrical power using a generator. Wind turbine power produces no emissions or pollutants during operation while reducing reliance on non-renewable resources.

- Electrolyzer stack: This is the location of the electrochemical conversion process for hybrid renewable-to-hydrogen, performed in an electrolysis cell with a proton exchange membrane (PEM) between a graphite-felt anode and a carbon cathode. Renewable electricity from wind and solar energy drives biomass electrolysis, producing hydrogen that can meet fuel demands or can be stored in a hydrogen storage system for later use.

- Biomass: Biomass fuel produces renewable hydrogen through electrolysis by converting organic materials, such as forestry residues or dedicated energy crops, into native biomass powder. The produced hydrogen is known as green hydrogen.

- Battery storage system (BESS): A battery storage system acts as a dynamic reservoir that stores excess electricity generated during periods of high production. The stored energy can be released during peak demand or when renewable sources are less active. Battery storage systems enhance grid stability, minimize energy wastage, and contribute significantly to the transition towards a sustainable and resilient energy ecosystem.

- Hydrogen storage system (HSS): This system uses tanks to store the produced hydrogen safely. During periods of increased energy demand or limited renewable sources, the stored hydrogen can be sold to meet this demand.

- Load: The system has two types of loads: hydrogen loads, such as fuel stations, and electrical loads. These loads are passive; therefore, they operate on a fixed schedule and cannot be effectively managed using an IEMS.
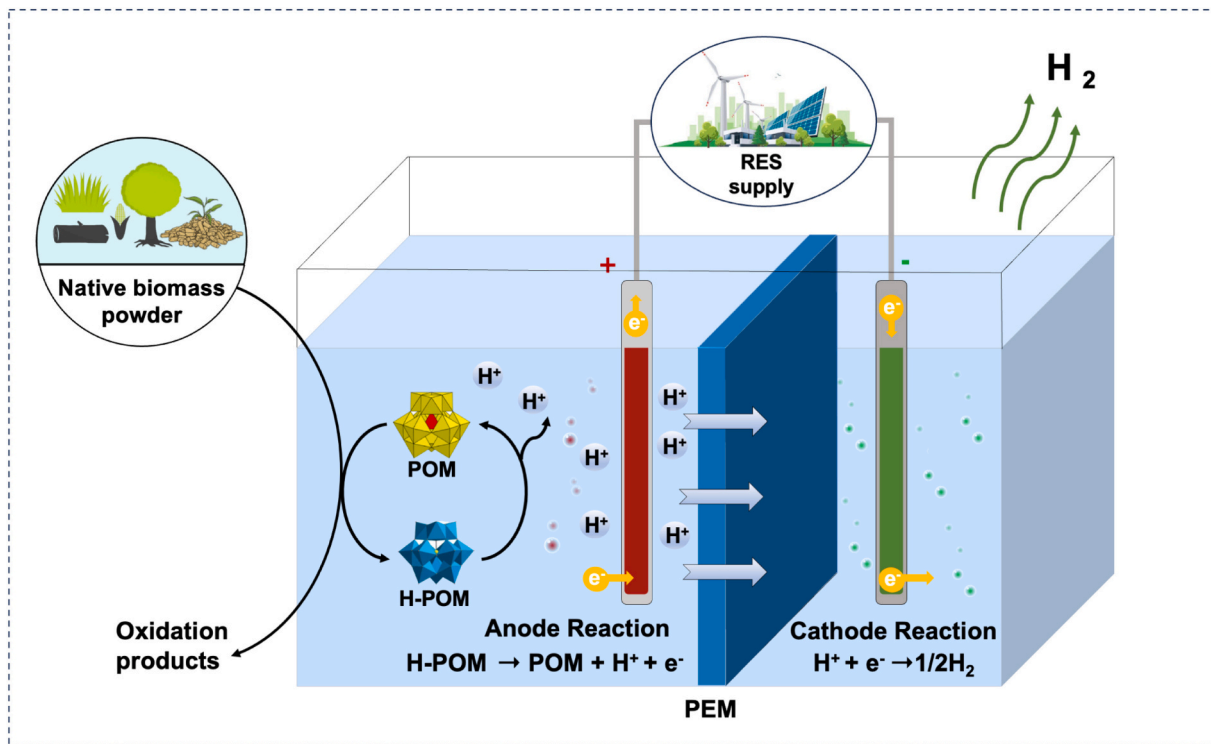
Fig. 3. The hydrogen production model.

- Integrated Energy Management System (IEMS): This efficiently manages energy consumption and reliably delivers power to meet energy needs. The IEMS facilitates the optimization of the operational timetable of diverse RESs, such as PV generation, wind turbines, biomass electrolyzers, BESSs, and HSSs, cohesively, ultimately leading to a reduction in operational expenses, mitigation of carbon emissions and enhancement of energy provision by the RES.

In an intelligent energy hub, the communication network facilitates the exchange of information between the IEMS, utility grid, and various devices. The input data conveyed to the IEMS encompass the duty cycle and energy consumption of hydrogen and electrical load, projected energy cost, state of energy of the BESS and HSS, and the anticipated output of the RES. Furthermore, the proposed algorithm was incorporated into an IEMS to scrutinize the essential information and energy consumption data and optimize the device operation schedule. Accordingly, the IEMS dispatches control signals to all devices for planned operation. As an active consumer, the IEH can purchase or sell energy from/to the utility grid: the utility grid, RES, and storage capacity of the BESS to supply electrical loads. Hydrogen from a biomass electrolyzer stack can be utilized at a fuel station or stored in the HSS. Furthermore, the surplus energy obtained from the RES and BESS can be sold back to the grid anytime for profit. The proposed IEH is a 24-hour MILP problem divided into 24 h intervals. The mathematical model and objectives of each IEH component are described below.

2.1. Green hydrogen production from RES modeling

The electrolysis process, as applied in an electrolyzer cell, facilitates the production of green hydrogen from RESs. The cell is designed with a proton exchange membrane (PEM) positioned between a graphite-felt anode and a carbon cathode, as shown in Fig. 3 [51,33]. The production of green hydrogen through biomass electrolysis can be powered by wind and solar energy through DC electric potential. The aqueous polyoxometalate (POM), a notable and cost-effective water-soluble molecular metal-oxide cluster, has been employed as a catalyst and e-mediator

to expedite the oxidative depolymerization of biomass and e-extraction [17]. In the aqueous electrolyte containing polyoxometalate (POM), native biomass powders undergo direct oxidation to yield electrolytic H2 production while presenting enhanced thermodynamics at elevated electrolysis temperatures. The process commences with the oxidation of biomass by POM, forming a reduced POM complex (H-POM) at the anode, with water molecules serving as proton (H^+) donors in the process: *Biomass* + H_2O + *POM→Oxidative products* + *H* − *POM*. Then, the reduced H-POM can be easily reoxidized at the anode surface, releasing e^- and H^+ into the electrolyte based on the reaction:*H* − *POM→POM* + H^+ + e^-. Finally, the application of an electric field induces the liberation of H^+ across the proton exchange membrane. Subsequently, the liberated H^+unites with$e^-$from the external circuit, forming H2 at the cathode side:$H^+ + e^- \rightarrow \frac{1}{2}H_2$.

The electrolyzer cell voltage was modeled based on the temperature-dependent U-I relationship [1,33]. Specifically, the electrolyzer cell voltage $u_t^c$is sensitive to the electrolysis temperature T_t^c and current I_t^c, as shown in Eq. (1). On the right-hand side of Eq. (1), the first term is the reversible voltage, denoting the ideal minimum energy needed to depolymerize biomass and generate H2. The second term is the irreversible voltage to overcome the ohmic resistance of the electrolyte. A unit cell has a limited H_2 output; therefore, a stack embedding several$N_c$units in series should be built be built, which increases the electrolytic stack voltage u_t^{elz}, as shown in Eq. (2). Finally, the H2 production rate m_t^{elz} at interval t of an electrolyzer cell can be determined by the electrolysis efficiency η^{elz}, the electrolytic stack power consumption P_t^{elz}, and the heating value of H2 Q_{H_2}, as shown in Eq. (4). The WT and PV units provide power for the electrolytic stack of biomass electrolysis. Therefore, the electrochemical model for green hydrogen production can be formulated as follows:

$$u_t^c = \frac{\Delta G_{bio}}{zF} + \frac{a_1 + a_2 T_t^c}{A_c}I_t^c; \quad \forall t = 1, 2, ..., T \tag{1}$$

$$u_t^{elz} = N_c \cdot u_t^c; \quad \forall t = 1, 2, ..., T \tag{2}$$

$$P_t^{elz} = u_t^{elz} \cdot I_t^c; \quad \forall t = 1, 2, ..., T \tag{3}$$

$$m_t^{elz} = \frac{\eta^{elz} P_t^{elz}}{Q_{H_2}}; \quad \forall t = 1, 2, ..., T \tag{4}$$

where ΔG_{bio} signifies the alterations in the free Gibbs energy pertaining to the reaction of biomass electrolysis; z represents the quantity of e^- transferred per one mole of H2; F represent the constants of Faraday; a_1, a_2 are parameters that are related to the ohmic resistance; A_c represents the surface area of the electrode.

Fig. 3 illustrates the RESs used to generate a green hydrogen system for the IEH to meet its energy requirements. The WT and PV units provided power for the biomass electrolysis, ultimately facilitating green hydrogen production in the electrolyzer stack. The hydrogen generated can be conserved within the confines of a hydrogen storage tank (HST) to satisfy the subsequent fuel requirements of the fuel stations.

2.2. Integrated energy hub modeling

2.2.1. Grid modeling

An IEH can buy or sell energy on the energy market. Constraints such as physical grid limits and power agreements can limit electricity trade. IEHs must undertake grid modeling to better understand the limitations and opportunities of the energy market, enabling informed decisions and maximum trading potential. The instantaneous power that can flow from/to the utility grid to/from the IEH is upper bounded, as modeled in Eqs. (5) and (6). Owing to limitation Eq. (7), energy cannot be purchased or sold simultaneously. The grid model can be formulated as follows [52,53]:

$$0 \leq P_t^{G2I} \leq u_t^{G2I} \cdot \overline{P}^{G2I}; \quad \forall t = 1, 2, ..., T \tag{5}$$

$$0 \leq P_t^{I2G} \leq u_t^{I2G} \cdot \overline{P}^{I2G}; \quad \forall t = 1, 2, ..., T \tag{6}$$

$$0 \leq u_t^{G2I} + u_t^{I2G} \leq 1; \quad \forall t = 1, 2, ..., T \tag{7}$$

where P_t^{G2I} is the power purchased from the grid, P_t^{I2G} is the power sold back to the grid during interval t; u_t^{G2I} and u_t^{I2G} are the binary variables of the purchase and sell modes of the IEH with the utility grid at interval t, respectively. $\overline{P}^{G2I}$ and $\overline{P}^{I2G}$ are the maximum powers that can be purchased and sold between the IEH and utility grid, respectively.

2.2.2. PV system modeling

Practically, the electricity output of the PV setup during a defined interval t can be calculated by relying on meteorological predictions that offer pertinent data regarding solar irradiation, using the following mathematical formula [53]:

$$P_t^{PV} = v_t \cdot \eta^{PV} \cdot \overline{P}^{PV} \cdot \Delta\tau; \quad \forall t = 1, 2, ..., T \tag{8}$$

where P_t^{PV} is the PV output at interval t; v_t represents the solar irradiance at time interval t; η^{PV} is the conversion efficiency, and $\overline{P}^{PV}$ represents the peak PV power.

2.2.3. WT modeling

The analysis of the output power of a wind turbine for a specific wind speed (v) can be expressed as follows [54]:

$$P_t^{WT} = \begin{cases} 0 & v_t \leq v_{cut\,in} \\ \dfrac{v_t - v_{cut\,in}}{v_{rated} - v_{cut\,in}} P_{rated} & v_{cut\,in} \leq v_t \leq v_{rated} \\ P_{rated} & v_{rated} \leq v_t \leq v_{cut\,out} \\ 0 & v_t \geq v_{cut\,out} \end{cases} \tag{9}$$

where $v_{rated}, v_{cut\,in}, v_{cut\,out}$ are the rated, cut-in, and cut-out wind speeds of the WT, respectively. P_{rated} represents the nominal power of the WT.

2.2.4. BESS modeling

IEHs often integrate BESS owing to their economic and technical advantages. Depending on the operation mode, a BESS can function as a power source or a consumer. The rated power of a BESS is the limited amount of power that can be charged or discharged, as shown in the following equation Eqs. (10) and (11) [52,53]:

$$0 \leq P_t^{BESS,ch} \leq u_t^{BESS,ch} \cdot \overline{P}^{BESS,ch}; \quad \forall t = 1, 2, ..., T \tag{10}$$

$$0 \leq P_t^{BESS,dis} \leq u_t^{BESS,dis} \cdot \overline{P}^{BESS,dis}; \quad \forall t = 1, 2, ..., T \tag{11}$$

$$0 \leq u_t^{BESS,ch} + u_t^{BESS,dis} \leq 1; \quad \forall t = 1, 2, ..., T \tag{12}$$

where $P_t^{BESS,ch}$ and $P_t^{BESS,dis}$ represent the charging and discharging power at interval t; $u_t^{BESS,ch}$ and $u_t^{BESS,dis}$ are the binary variables representing the charging and discharging modes of the BESS at interval t; $\overline{P}_t^{BESS,ch}$ and $\overline{P}_t^{BESS,dis}$ are the maximum affordable charging and discharging powers of the BESS, respectively. Eq. (12) indicates that the BESS charging and discharging operations are mutually exclusive.

As shown in Eq. (13), ε_t^{BESS} is the state of energy (SOE) of the BESS during a given interval t which relies on ε_{t-1}^{BESS} during the previous interval, the amount of energy charged into the BESS, and the energy discharged back into the IEH, and the grid at interval t. BESS is limited by its depth of discharge (DOD) and maximum capacity, as shown in Eq. (14) [33,52,53]:

$$\varepsilon_t^{BESS} = \varepsilon_{t-1}^{BESS} + \left(\eta^{BESS} \cdot P_t^{BESS,ch} - \frac{P_t^{BESS,dch}}{\eta^{BESS}} \right) \cdot \Delta\tau / \overline{P}^{BESS}; \quad \forall t = 1, 2, ..., T \tag{13}$$

$$\left(1 - DOD^{BESS} \right) \cdot \overline{\varepsilon}^{BESS} \leq \varepsilon_t^{BESS} \leq \overline{\varepsilon}^{BESS}; \quad \forall t = 1, 2, ..., T \tag{14}$$

$$\varepsilon_1^{BESS} = \varepsilon_T^{BESS} = \overline{\varepsilon}^{BESS} \tag{15}$$

where η^{BESS} is the charge/discharge efficiency of the BESS; DOD^{BESS} is the BESS depth of discharge; $\overline{\varepsilon}^{BESS}$ is the maximum capacity. As per Eq. (15), this study assumes the energy contained within the BESS is configured to its utmost capacity during the initial ε_1^{BESS} and final intervals of the scheduling period ε_T^{BESS} [52].

2.2.5. HSS modeling

HSS should store the produced hydrogen safely and provide the required hydrogen to meet the hydrogen demand. In Eq. (16), the hydrogen outflow rate of HSS equals the hydrogen demand of IEH at interval t. Eq. (17) indicates that the SOE of the HSS at interval t equals the total remaining energy in the previous interval and the hydrogen gap between production and consumption. The hydrogen stored in the HSS at interval t, denoted by H_t^{HSS}. Eq. (18) models the SOE of the HSS at interval t as a function of hydrogen stored in the HSS at interval t and the maximum energy stored in the HSS. The SOE of the HSS at interval t should be constrained within its physical lower and upper bounds to avoid over-charging and over-discharging, as shown in Eq. (19) [55]. The energy contained within the HSS is configured to maximum capacity at the start and the end of the scheduling period, as shown in Eq. (20). Therefore, HSS is represented as follows [38,56]:

$$m_t^{HSS} = H_t^{demand}; \quad \forall t = 1, 2, ..., T \tag{16}$$

$$H_t^{HSS} = H_{t-1}^{HSS} + m_t^{elz} - m_t^{HSS}; \quad \forall t = 1, 2, ..., T \tag{17}$$

$$\varepsilon_t^{HSS} = \frac{H_t^{HSS}}{\overline{H}^{HSS}}; \quad \forall t = 1, 2, ..., T \tag{18}$$

$$\underline{\varepsilon}^{HSS} \leq \varepsilon_t^{HSS} \leq \overline{\varepsilon}^{HSS}; \quad \forall t = 1, 2, \dots, T \tag{19}$$

$$\varepsilon_1^{HSS} = \varepsilon_T^{HSS} = \overline{\varepsilon}^{HSS} \tag{20}$$

where m_t^{HSS}, H_t^{demand} represent the output of HSS and the hydrogen demand at time t, respectively; ε_t^{HSS} is the SOE of the HSS at interval t; $\overline{H}^{HSS}$ is the maximum energy stored in the HSS; $\underline{\varepsilon}^{HSS}$ and $\overline{\varepsilon}^{HSS}$ represent the minimum and maximum SOE of the HSS, respectively.

2.2.6. Energy balance

The proposed IEH framework must satisfy all energy requirements within a designated period and maintain the energy balance using the following equation:

$$P_t^{G2I} + P_t^{PV} + P_t^{WT} + P_t^{BESS,dis} = P_t^{load} + P_t^{I2G} + P_t^{elz} + P_t^{BESS,ch};$$
$$\forall t = 1, 2, \dots, T \tag{21}$$

where P_t^{load} is the electricity load demand at interval t.

2.3. Objective function

In this study, the optimization of the BESS and HSS in the IEH was achieved by maximizing the use of underutilized RESs. Multi-objective functions aim to achieve optimal results in terms of economy, emissions, and energy balance ability. The multi-objective optimization problem of the IEH problem can be formulated as follows:

$$minf(x) = [f_1(x), f_2(x), f_3(x)] \tag{22}$$

where $f(x)$ is the vector of the three objective functions, and x is the vector of the decision variables defined below:

$$x = \left\{ \begin{array}{l} P_t^{G2I}, P_t^{I2G}, P_t^{BESS,dis}, P_t^{BESS,ch}, u_t^{G2I} \\ u_t^{I2G}, u_t^{BESS,dis}, u_t^{BESS,ch}, m_t^{elz}, m_t^{HSS} \end{array} \right\}; \\ \forall t = 1, 2, \dots, T \tag{23}$$

The IEH problem involves three objective functions that aim to minimize operational costs, carbon emissions, and the energy export index. This process is described as follows:

2.3.1. Minimize operation cost

The first objective of the IEH is to minimize the operation cost shown in Eq. (24). The cost of using an IEH includes the operational costs of the equipment (Eq. (25)), the grid taxes (Eq. (26)), and the energy cost (Eqs. (27)–(29)). The cost of purchasing fuel is the cost of purchasing the biomass for hydrogen electrolysis (Eq. (27)). The cost of buying energy is the cost of purchasing energy from the utility grid to meet the load demand (Eq. (28)), and the sale of energy includes revenue from the hydrogen produced by the electrolyzer and electricity provided by the RES to the public grid (Eq. (29)). The revenue from selling hydrogen depends on the volume of hydrogen, whereas the price of hydrogen is assumed to be constant. However, power sales are contingent on the hourly electricity price and the excess production of renewable energy sources. The grid tax is based on the consumption and equilibrium tariffs, including transmissions without transformers, systems, consumption, or carbon taxes (Eq. (30)) [23]. The RES tax is based on production and equilibrium tariffs, including induction, balance, and commission balance tax ((Eq. (31)) [23].

$$minf_1 = \sum_{t=1}^{T} Cost_t^{eq} + Cost_t^{tax} + Cost_t^{fuel} + Cost_t^{buy} - Cost_t^{sell} \tag{24}$$

$$Cost_t^{eq} = \lambda^{PV} \cdot P_t^{PV} + \lambda^{WT} \cdot P_t^{WT} + \lambda^{BESS} \cdot P_t^{BESS} + \lambda^{elz} \cdot P_t^{elz} + \lambda^{HSS} \cdot m_t^{HSS} \tag{25}$$

$$Cost_t^{tax} = tax^{RES}(P_t^{PV} + P_t^{WT}) + tax^{Grid} \cdot P_t^{G2I} \tag{26}$$
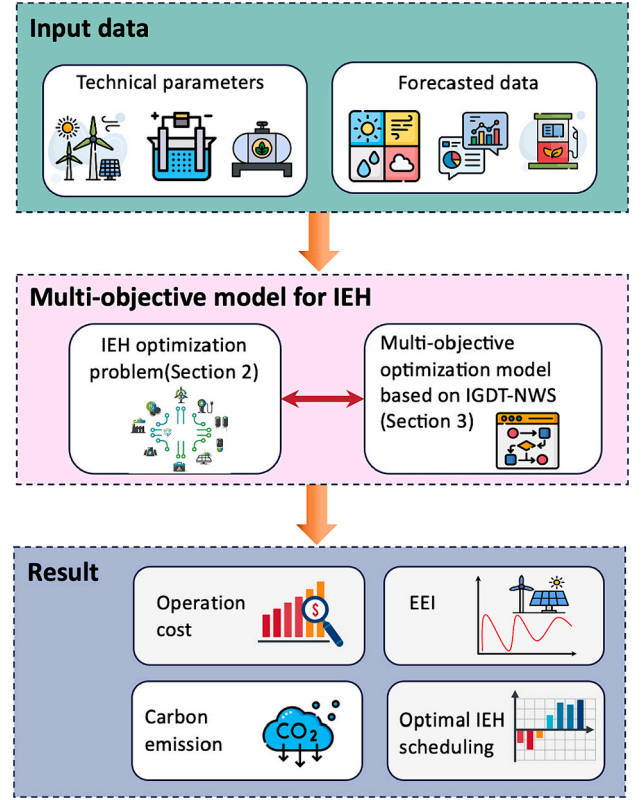

Fig. 4. Flowchart of the proposed methodology for multi-objective IEH framework.

$$Cost_t^{fuel} = Cost_t^{biomass} = \lambda_t^{biomass} \cdot m_t^{elz} \tag{27}$$

$$Cost_t^{buy} = \lambda_t^e \cdot P_t^{G2I} \tag{28}$$

$$Cost_t^{sell} = \lambda_t^e \cdot P_t^{I2G} + \lambda_t^{H_2} \cdot m_t^{H2,sell} \tag{29}$$

$$tax_t^{Grid} = tax_{twt} + tax_{st} + tax_{ct} + tax_{cbt} + tax_{CO_2} \cdot CO_{2_{grid}} \tag{30}$$

$$tax_t^{RES} = tax_{it} + tax_{bt} + tax_{cbt} \tag{31}$$

where λ^{PV}, λ^{WT}, λ^{BESS}, λ^{elz} are the equipment operating cost of PV, WT, BESS, and electrolyzer, respectively; λ_t^e is the electricity cost at interval t; λ^{H_2}, $\lambda^{biomass}$ represent hydrogen selling price and biomass fuel cost, respectively; $tax_{twt}, tax_{st}, tax_{ct}, tax_{cbt}, tax_{CO_2}$ are the tax of transmission without transformer, system, consumption, commission balance and carbon, respectively; tax_{it}, tax_{bt} represent the tax of induction and balance; $CO_{2_{grid}}$ is the carbon emission of the grid.

2.3.2. Minimize carbon emission

The objective function in Eq. (32) aims to minimize the carbon emissions of IEH [23]. An IEH purchases power from the grid to meet the load demand and charging, which leads to harmful emissions.

$$minf_2 = \sum_{t=1}^{T} \sigma^{CO_2} \cdot P_t^{G2I} \tag{32}$$

where σ^{CO_2} represent the CO_2 emission coefficient.

2.3.3. Minimize EEI

The energy export index (EEI) was used to determine the energy balance in the grid [57]. This index measures the amount of energy exported to the grid. A lower EEI indicates a better balance between

energy exports, which reflects the grid's ability to withstand fluctuations and disruptions. Therefore, a lower EEI indicates better grid resilience. The objective f_3 aims to minimize the EEI, which can be computed as follows:

$$min f_3 = \frac{\sum_{t=1}^{T} P_t^{I2G}}{\sum_{t=1}^{T} P_t^{gen}} \tag{33}$$

where P_t^{gen} represent the total power generated from RESs at interval t.

3. Proposed methodology

This study applies the proposed information gap decision-theory-based normalized weighted-sum approach (IGDT-NWS) to the IEH optimization problem with multi-objectives. An overview of the proposed method for the IEH framework with multiple objectives is presented in Fig. 4.

3.1. The normalized weighted-sum approach (NWS)

The NWS method uses different weighting coefficients for each objective function in this study. This method is a popular approach for solving multi-objective optimization problems. This involves combining all functions into one composite objective function. The following equations illustrate this:

$$Minimize \sum_{i=1}^{k} \omega_i \cdot f_i(x); \quad \forall i = 1, 2, \dots, k$$
$$s.t \quad x \in \Omega$$
$$\omega_i \geq 0 \tag{34}$$
$$\sum_{i=1}^{k} \omega_i = 1$$

Normalizing objectives is essential to obtain *pareto optimal* solutions that reflect the weights the "decision maker assigns." The normalization factor θ is expressed as follows [58]:

$$\theta = \frac{1}{f^* - f_*} \tag{35}$$

This normalization formula depends on the distinctions between the optimal values at the Nadir and Utopia points [58]. The "Pareto optimal" set represents the range within which the optimal objective function differs. The Utopia point f_* is achieved through the independent minimization of each objective function while subject to the original constraints (1)–(21), which present the optimal ideal value for each objective. However, the anti-ideal value of the objective function is achieved by maximizing each function independently while subject to the original constraints (1)–(21), resulting in a Nadir point f^*. Hence, the normalization factors for the three objective functions can be expressed as follows:

$$\theta_i = \frac{1}{f_i^* - f_{i*}}; \quad \forall i = 1, 2, 3 \tag{36}$$

Therefore, the formulations of Eq. (34) can be rewritten as an aggregated objective function as follows:

$$Minimize \quad \omega_1 \cdot \theta_1 \cdot f_1 + \omega_2 \cdot \theta_2 \cdot f_2 + \omega_3 \cdot \theta_3 \cdot f_3 \tag{37}$$

where ω_1, ω_2, and ω_3 denote the weights assigned to the three objective functions. The objective function can be represented in detail as follows:

$$Minimize \left[\omega_1 \cdot \frac{f_1}{f_1^* - f_{1*}} + \omega_2 \cdot \frac{f_2}{f_2^* - f_{2*}} + \omega_3 \cdot \frac{f_3}{f_3^* - f_{3*}} \right] \tag{38}$$

Uncertainty horizon

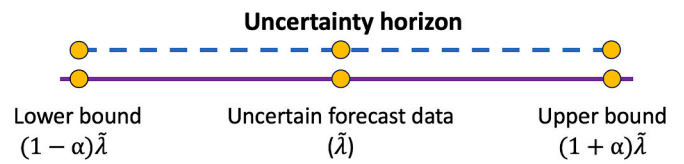| Lower bound | Uncertain forecast data | Upper bound |
| $(1 - \alpha)\tilde{\lambda}$ | $(\tilde{\lambda})$ | $(1 + \alpha)\tilde{\lambda}$ |

Fig. 5. Concept of uncertainty modeling.

3.2. IGDT method

This study uses the IGDT method to model the uncertain RES output, energy price, and hydrogen and electricity demand. Generally, the IGDT is a non-fuzzy and non-probabilistic method that does not require information regarding the probability distribution of uncertain parameters [59]. This method can be used from either a risk-seeking or a risk-averse perspective. A hybrid version of the two strategies is proposed to consider their advantages for practical and near-realistic system modeling, allowing the operator to choose the appropriate strategy for operation scheduling goals. In the following subsections, we describe the principles and formulation of IGDT.

3.2.1. Uncertainty modeling

The theoretical framework of the IGDT encompasses an array of uncertainty models. The Fractional error approach, which is one of the most commonly used uncertainty models, is mathematically described using Eq. (39) [42,60]. This model indicates that the uncertain variable deviates less from the forecasted value than the scalar parameter α. The uncertainties in the operation system of the input parameters can be considered as a set of U.

$$U(\alpha, \lambda_t) = \left\{ \lambda_t : \left| \frac{\lambda_t - \tilde{\lambda}_t}{\tilde{\lambda}_t} \right| \leq \alpha \right\}; \quad \forall t = 1, 2, \dots, T \tag{39}$$

where $\tilde{\lambda}_t$ represents the uncertain forecast data at interval t, respectively. The uncertainty modeling concept in IGDT is represented graphically in Fig. 5. The confidence interval increases with an increase in the predicted value.

In this study, the uncertainties include renewable energy source output P^{PV}, P^{WT}, electricity P^{load} and hydrogen demand m^{demand}, and energy price λ^e. Regarding this model, $\alpha^{load}, \alpha^H, \alpha^e, \alpha^{PV}, \alpha^{WT}$ are the uncertainty horizons of P^{load}, m^{demand}, λ^e, P^{PV}, P^{WT}, respectively. The uncertainty horizon for each input uncertainty data can be rewritten according to Eq. (39) as follows [49]:

$$\left(1 - \alpha^{load}\right)\tilde{P}_t^{load} \leq P_t^{load} \leq \left(1 + \alpha^{load}\right)\tilde{P}_t^{load} \tag{40}$$

$$\left(1 - \alpha^H\right)\tilde{H}_t^{demand} \leq H_t^{demand} \leq \left(1 + \alpha^H\right)\tilde{H}_t^{demand} \tag{41}$$

$$\left(1 - \alpha^e\right)\tilde{\lambda}_t^e \leq \lambda_t^e \leq \left(1 + \alpha^e\right)\tilde{\lambda}_t^e \tag{42}$$

$$\left(1 - \alpha^{PV}\right)\tilde{P}_t^{PV} \leq P_t^{PV} \leq \left(1 + \alpha^{PV}\right)\tilde{P}_t^{PV} \tag{43}$$

$$\left(1 - \alpha^{WT}\right)\tilde{P}_t^{WT} \leq P_t^{WT} \leq \left(1 + \alpha^{WT}\right)\tilde{P}_t^{WT} \tag{44}$$

3.2.2. Risk-Averse Strategy (RA)

From a risk-aversion strategy, the IGDT methodology enhances the uncertainty horizon to achieve the objective value that does not exceed the critical value. This IGDT strategy is recognized as a robustness function and can be delineated by the following formulation [42,2]:

$$max \quad \alpha(X, \lambda) \tag{45}$$

Subject to:

$$f(X, \lambda) \leq f_{cr}; \quad \forall \lambda \in U \tag{46}$$

$$g(X, \lambda) = 0; \quad \forall \lambda \in U \tag{47}$$

$$h(X, \lambda) \leq 0; \quad \forall \lambda \in U \tag{48}$$

$$f_{cr} = (1 + \beta)\bar{f}; \quad \forall \lambda \in U \tag{49}$$

where $\bar{f}$ is the optimal value if the uncertain input data match the forecast data, f_{cr} represents the maximum tolerable objective value, and β denotes the critical deviation factor. The main aim of a risk-averse strategy is to establish decision variables that mitigate the risks associated with uncertain input data. In other words, the risk-averse IGDT ensures that the minimum requirements are satisfied [42,59]. Additionally, lower critical objective values decrease the robustness horizon.

The risk-averse strategy applied in this study maximizes the uncertainty horizon (or robustness horizon) while ensuring that the IEH operation cost does not exceed a critical operation cost. In this decision-making mode, the IEH operation cost is not worse than the given target operating cost for the worst realization of uncertain input. To ensure that it is better than the critical operation cost, $(1 + \alpha^{load})\tilde{P}^{load}$, $\alpha^H(1 + \alpha^H)\tilde{H}^{demand}$, $(1 + \alpha^e)\tilde{\lambda}^e$ are the worst realization of electricity, hydrogen demands, and electricity prices, respectively, as shown in Eqs. (53)–(55). At the same time, the worst PV and WT power realizations are $(1 - \alpha^{PV})\tilde{P}^{PV}$, $(1 - \alpha^{WT})\tilde{P}^{WT}$, as shown in Eqs. (56), (57). This strategy hedges IEH operators against unfavorable demands, RES output, and electricity price deviations. Based on the explanations above, the risk-averse strategy of IGDT can be expressed as follows [42,45]:

$$max(\alpha) \tag{50}$$

$$\alpha = min(\alpha^{load}, \alpha^H, \alpha^e, \alpha^{PV}, \alpha^{WT}) \tag{51}$$

Subject to:

$$f_1 \leq (1 + \beta) \cdot \bar{f} \tag{52}$$

$$P_t^{load} = (1 + \alpha^{load})\tilde{P}_t^{load} \tag{53}$$

$$H_t^{demand} = (1 + \alpha^H)\tilde{H}_t^{demand} \tag{54}$$

$$\lambda_t^e = (1 + \alpha^e)\tilde{\lambda}_t^e \tag{55}$$

$$P_t^{PV} = (1 - \alpha^{PV})\tilde{P}_t^{PV} \tag{56}$$

$$P_t^{WT} = (1 - \alpha^{WT})\tilde{P}_t^{WT} \tag{57}$$

3.2.3. Risk-Seeker Strategy (RS)

In the risk-seeking strategy, the target cost is pre-established, and the primary objective is to ascertain an uncertainty horizon (or opportunity horizon) that renders the attainment of f_{tg} feasible. The most favorable deviations of the uncertain input data will ensure that the objective function value does not exceed the target f_{tg}. The risk-seeking strategy is modeled as follows [42,45]:

$$min \; \alpha(X, \lambda) \tag{58}$$

Subject to:

$$f(X, \lambda) \leq f_{tg}; \quad \forall \lambda \in U \tag{59}$$

$$g(X, \lambda) = 0; \quad \forall \lambda \in U \tag{60}$$

$$h(X, \lambda) \leq 0; \quad \forall \lambda \in U \tag{61}$$

$$f_{tg} = (1 - \rho)\bar{f}; \quad \forall \lambda \in U \tag{62}$$

where f_{tg} represents the target objective value and ρ denotes the critical deviation factor. In this strategy, the optimistic risk-seeking decision-
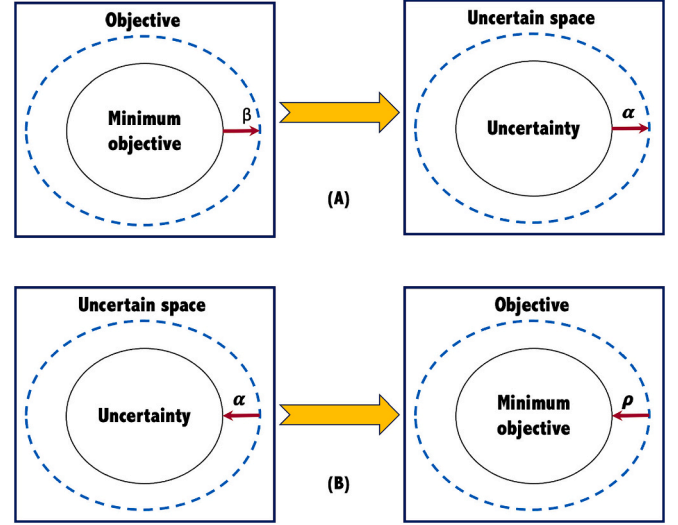

Fig. 6. Concepts of (A) risk-averse strategy and (B) risk-seeker strategy.

maker hopes to benefit from desirable deviations of uncertain input data from forecasted values. Similar to the risk-averse strategy, lower f_{tg} results in lower of opportunity horizon values.

The risk-seeking strategy applied in this study minimizes the uncertainty horizon (or the opportunity horizon) to achieve a target operation cost. $(1 - \alpha^{load})\tilde{P}^{load}$, $(1 - \alpha^H)\tilde{H}^{demand}$, $(1 - \alpha^e)\tilde{\lambda}^e$ must be the best realizations of electricity and hydrogen demands and energy prices to achieve a target operating cost, as shown in Eqs. (66)–(68). $(1 + \alpha^{PV})\tilde{P}^{PV}$, $(1 + \alpha^{WT})\tilde{P}^{WT}$ are the best realizations of PV and WT power, respectively, as shown in Eqs. (69)–(70). In this strategy, the IEH operator aims to increase profits by taking advantage of favorable fluctuations in demand, generation RES, and energy prices. According to the given explanations, the risk-seeking strategy of IGDT can be expressed as follows [42,45]:

$$min(\alpha) \tag{63}$$

$$\alpha = max(\alpha^{load}, \alpha^H, \alpha^e, \alpha^{PV}, \alpha^{WT}) \tag{64}$$

Subject to:

$$f_1 \leq (1 - \rho) \cdot \bar{f} \tag{65}$$

$$P_t^{load} = (1 - \alpha^{load})\tilde{P}_t^{load} \tag{66}$$

$$H_t^{demand} = (1 - \alpha^H)\tilde{H}_t^{demand} \tag{67}$$

$$\lambda_t^e = (1 - \alpha^e)\tilde{\lambda}_t^e \tag{68}$$

$$P_t^{PV} = (1 + \alpha^{PV})\tilde{P}_t^{PV} \tag{69}$$

$$P_t^{WT} = (1 + \alpha^{WT})\tilde{P}_t^{WT} \tag{70}$$

In Fig. 6A, the decision-maker adopts a pessimistic approach by increasing the minimum objective to account for a more significant portion of the uncertain space. However, in Fig. 6B, the decision maker is optimistic about the uncertainties of the system. The objective value decreases as the uncertain variables deviate favorably from the forecast value.

3.3. Application of the IGDT-NWS

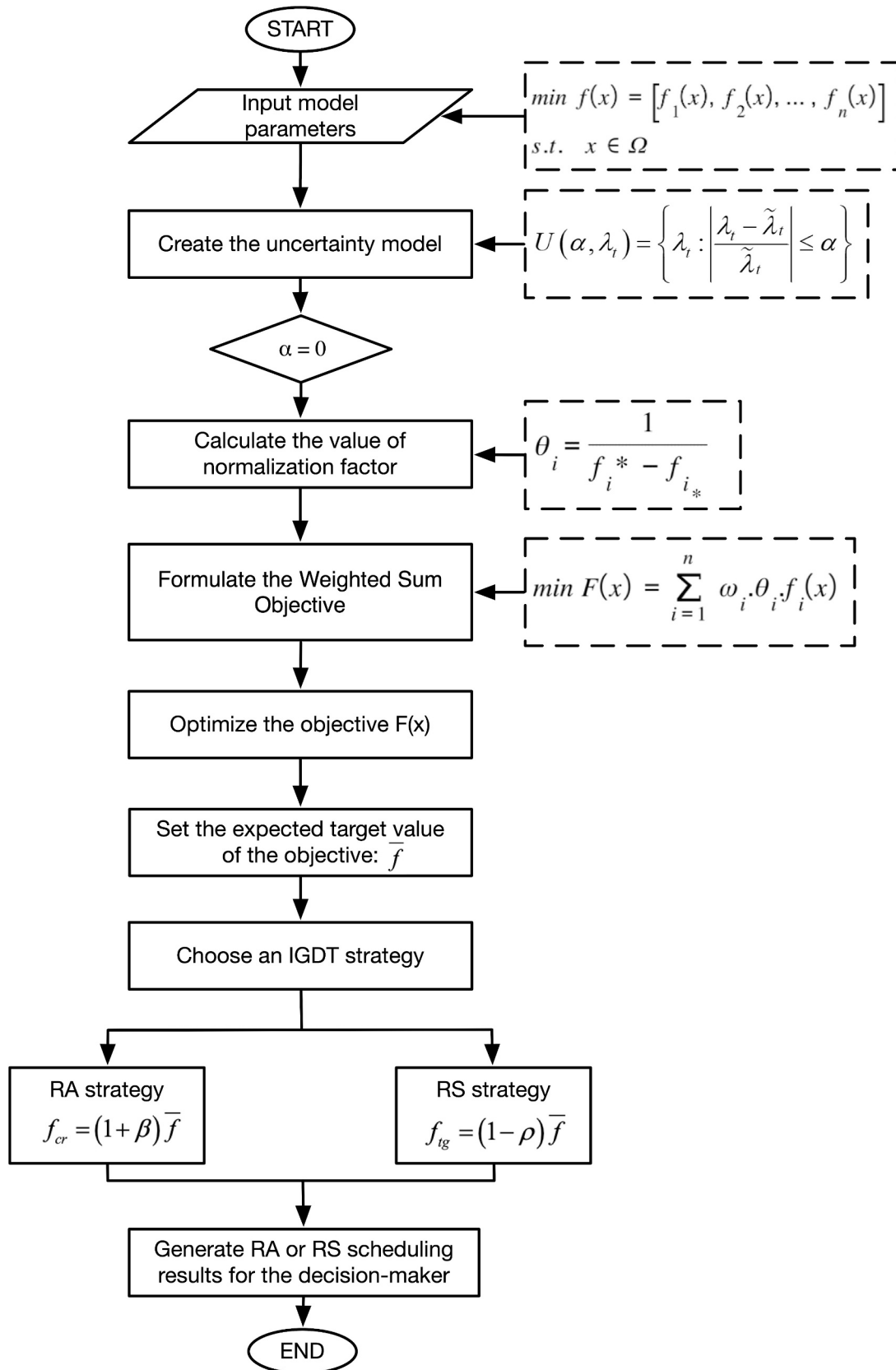An overview of the implementation of the IGDT-NWS algorithm for the proposed IEH model is illustrated in Fig. 7.

START

Input model parameters

$$min \ f(x) = \left[f_1(x), f_2(x), \dots, f_n(x) \right]$$
$$s.t. \quad x \in \Omega$$

Create the uncertainty model

$$U(\alpha, \lambda_t) = \left\{ \lambda_t : \left| \frac{\lambda_t - \tilde{\lambda}_t}{\tilde{\lambda}_t} \right| \le \alpha \right\}$$

$\alpha = 0$

Calculate the value of normalization factor

$$\theta_i = \frac{1}{f_i^* - f_{i_*}}$$

Formulate the Weighted Sum Objective

$$min \ F(x) = \sum_{i=1}^{n} \omega_i . \theta_i . f_i(x)$$

Optimize the objective F(x)

Set the expected target value of the objective: $\overline{f}$

Choose an IGDT strategy

RA strategy
$$f_{cr} = (1 + \beta)\overline{f}$$

RS strategy
$$f_{tg} = (1 - \rho)\overline{f}$$

Generate RA or RS scheduling results for the decision-maker

END
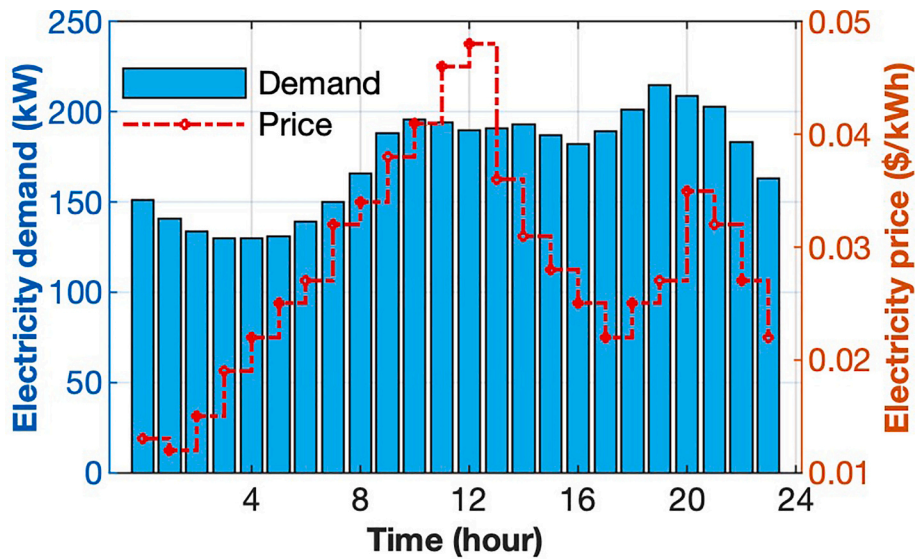
Fig. 7. Flowchart of the proposed IGDT-NWS.

Fig. 8. Day-ahead hourly electric price and load demand.

The IGDT-NWS model is conducted according to the following steps:

Step 1: Prepare classified input information as known and predicted data.

- Available information: operation equipment cost, taxes, biomass electrolyzers, battery, and hydrogen storage system parameters.
- Predicted data: PV and WT generation, electricity and hydrogen demand, electricity price.

Step 2: Create the uncertainty model (Eq. (40)–(44)).

Step 3: Set $\alpha = 0$. Run the base model to calculate the normalization factor θ_i for each objective (defined in Section 2).

Step 4: Formulate combining all functions into one composite objective $F(x)$ (Eq. (38)).

Step 5: Optimize the objective $F(x)$.

Step 6: Set the optimal value of objectives in the base model as the expected target value $\bar{f}$.

Step 7: Choose to apply one of the two strategies of the IGDT method: Set target deviation factor and establish optimal model under RA-Strategy or RS-Strategy.

- *Risk-Averse Strategy:*
  - Set the critical deviation factor β.
  - Base model with constraints Eq. (52)–(57).
- *Risk-Seeker Strategy:*
  - Set the critical deviation factor ρ.
  - Base model with constraints Eq. (65)–(70).

Step 8: Determine the optimal objective value and operation scheduling for IEH.

4. Simulation results

This section presents various simulation cases for validating the proposed paradigm of the IEH model. The deterministic model considers the day-ahead data of the RES output, energy price, and energy demand.
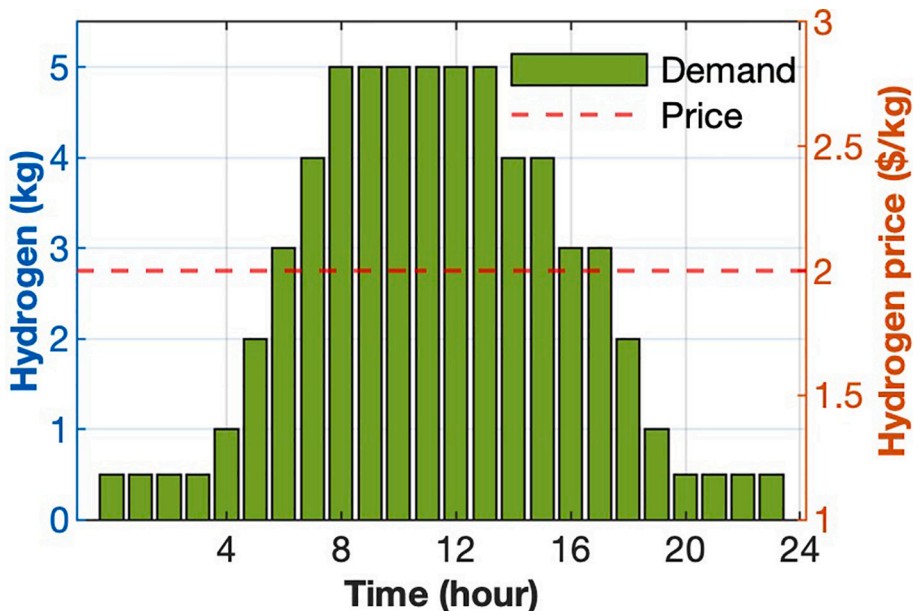

Fig. 9. Day-ahead hourly hydrogen price and demand.

Table 2
Data of BESS and HSS data.

BESS		HSS	
Parameter	Value	Parameter	Value
$\overline{P}^{BESS}$	220 kWh	$\overline{H}^{HSS}$	20 (kg)
$\overline{P}^{BESS,ch}, \overline{P}^{BESS,dis}$	60 kW/60 kW	$\overline{\epsilon}^{HSS}$	0.9
η^{BESS}	0.93	$\underline{\epsilon}^{HSS}$	0.2
DOD^{BESS}	0.70		
$\overline{\epsilon}^{BESS}$	0.95		

Table 3
Technical parameters of the biomass electrolyzer.

Electrolyzer stack	
Parameter	Value
A_c	0.286 (m^2)
a_1/a_2	7.2 * 10^{-3}/−1.5774 * 10^{-5}
$\overline{I}^c/\underline{I}^c$	804 A/0 A
N_c/η^{elz}	4000/0.6
$\overline{P}^{elz}$	500 (kW)
Q_{H_2}	39.72 (kWh/kg)
T^c	313 K
ΔG_{bio}	2.894 × 10^4 (J/mol)

The IGDT model considers these factors to be uncertain. The simulations were performed for 24 h with a 1-hour time step (0,00−23,00 h), resulting in a daily scheduling process with 24 intervals. The formulation of the IEH system was solved using a CPLEX solver in GAMS.

4.1. Input data

The proposed model was evaluated using a typical IEH as shown in Fig. 1. The history of electricity prices and daily electrical demand was based on data from [61], as shown in Fig. 8.

Fig. 9 shows the daily hydrogen demand profile of GreenLab Skive in Denmark, ranging from 0 % to 25 % [23]. In addition, the price of green hydrogen, based on a survey of the SG H2 Energy, is 2 ($/kg) [62]. The type of battery used in the IEH is a Li-ion battery, and the parameters are listed in Table 2, which are taken from [2,45,52]. Similarly, the HSS parameters in Table 2 were obtained from [33]. The technical parameters of the electrolyzer stack are listed in Table 3 [33,63,38]. An IEH can provide the requisite electrical energy to cater to the loads through renewable energy sources or buy from the power grid. Fig. 10 shows the forecast data for the RES output collected from [64]. The expenses for electric grid taxes and operational costs, including taxes, are listed in Tables 4 and 5 [2,7,23,45]. The cost of purchasing biomass fuel for biomass electrolysis to produce hydrogen is 0.3 ($/kg$_{H2}$) [65].
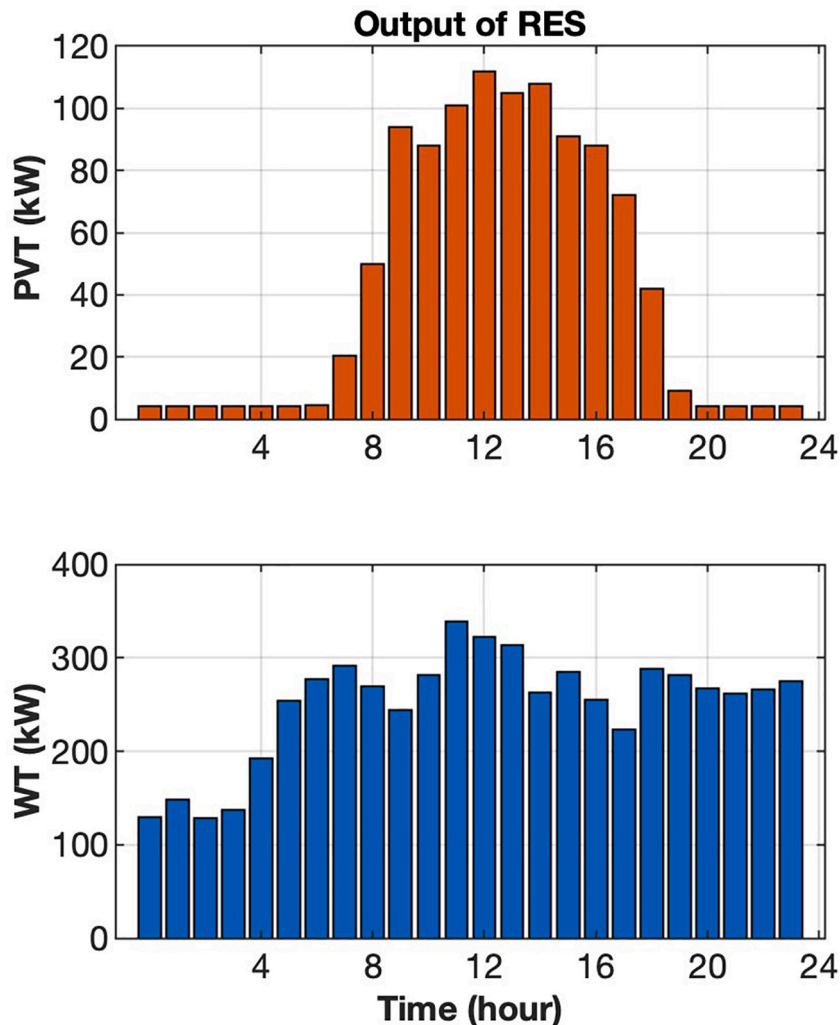

Fig. 10. Day-ahead hourly output of RESs.

Table 4

The energy production taxes.

Tax			
Consumption tariff	Transmission without transformer	tax_{twt}	0.66 ($/MWh)
	System	tax_{st}	0.82 ($/MWh)
Production tariffs	Consumption	tax_{ct}	0.03 ($/MWh)
	Induction	tax_{it}	0.04 ($/MWh)
	Balance	tax_{bt}	0.06 ($/MWh)
Equilibrium tariffs	Commission balance	tax_{cbt}	0.01 ($/MWh)
Carbon tax		tax_{CO_2}	0.003 ($/kg)

Table 5

The operation cost of the system.

Operation cost	
Parameter	Value
λ^{PV}	0.001 ($/kWh)
λ^{WT}	0.008 ($/kWh)
λ^{BESS}	0.002 ($/kWh)
λ^{elz}	0.001 ($/kWh)
λ^{HSS}	0.001 ($/kg)
λ^{H_2}	2($/kg)
$\lambda^{biomass}$	0.3 ($/kg H2)

Table 6

Single-objective values.

Case	f_1	f_2	f_3
Case 1: Minimize operation cost	2.5613	108.3702	0.0417
Case 2: Minimize carbon emission	6.7275	103.6842	0.0206
Case 3: Minimize EEI	8.1788	104.1164	0.0172

	Case 1	Case 2	Case 3
Total power bought from grid (kW)	1490.0342	1425.6045	1431.547
Total power sold to grid (kW)	292.723	144.7575	120.6736

4.2. Optimization of IEH without considering uncertainties

4.2.1. Single-objective optimization

In this section, an analysis is conducted to consider individually minimizing the operational cost, carbon emissions, and energy export index objectives. This approach aims to evaluate the conflicting nature of the various objectives. Notably, the results show that achieving one objective at a minimum may result in another objective having a high value. The values of the objective functions in the three single-objective cases are listed in Table 6 and visually presented in Fig. 11.

Figs. 12, 13, 14, and 15 present the scheduling profile of the IEH for each single-objective optimization case, which clearly shows their contradictory nature. In the first case, the objective is to minimize the operating costs. Most of the time, the operator does not use the BESS to avoid incurring additional operating costs. The BESS operates for several hours and recharges entirely at the end of the day. This leads to an increase in the EEI when the energy generated from the RES is sold to the market, potentially causing an imbalance in the IEH power grid. Furthermore, during high-demand intervals (5:00–18:00 h), the IEH must continuously purchase electricity from the grid, causing the emission value to increase. In the second case, BESS and HSS are used to reduce carbon emissions by utilizing electricity generated by RES instead of grid electricity. The amount of electricity purchased from the grid decreased by approximately 4.32 % compared to the first case. In the final case, the BESS and HSS are fully utilized to balance the energy in the IEH, thereby increasing the ability of the IEH to withstand load fluctuations. Consequently, the EEI is significantly reduced by

approximately 58.75 % compared with the first case. In addition, low power exports to the grid have resulted in a significant increase in operating costs. From the results of the three cases, it is evident that by considering only one objective, the values of the other objectives should be considered more comprehensively. Therefore, this study proposes a multi-objective IEH model with mutually binding goals.

The operating conditions of the electrolyzer stack used to produce green hydrogen are shown in Fig. 16. It includes the controlled electrolysis current and voltage and is measured at 24-hour intervals. Case 1 can maintain relatively stable electrolysis currents compared to case 2,3 for H2 production to avoid high fluctuations and reduce the associated life degradation cost of the electrolyzer. Additionally, the HSS offers high operation flexibility for IEH to deal with redundant/deficit RES generation, and BESS can help mitigate electrolysis current fluctuations during the H2 production process. In all three cases, abundant power from RES provides the required activation energy for breaking strong atomic bonds and accelerating H2 production rates during hours 5–18. At this interval, the electrolysis voltage is much higher to support the oxidative depolymerization of biomass. Fig. 17 shows the H2 production rate of the IEH for each case. The electrolysis voltage increases with increasing current, whereas the temperature remains constant. The HSS provides a large storage capacity for wind turbines and photovoltaic energy in the form of hydrogen energy, and actions of the BESS help manage the electrolysis current fluctuations. Renewable power from wind turbines is primarily used to drive biomass electrolysis during periods of low demand. Compared to other methods, the first case, with the aim of achieving the operation cost objective, helps to coordinate better the storage, conversion, and trading of hydrogen and electricity.

4.2.2. Multi-objective optimization

In this study, the proposed multi-objective IEH framework aims to simultaneously minimize operation cost, carbon emission, and energy export index. The proposed NWS is applied to the multi-objective optimization of IEH. A detailed result of the application of the proposal is presented in the subsection. Table 7 shows the results of cases using different weighting factors for each objective function.

For f_1, the values were the lowest in cases 1 when the weighting factors were set to the highest. For f_2 and f_3, the minimum value is achieved when the weighting factor of both objective functions is highest, as in cases 4 and 6. The objective value changed significantly between the minimum and maximum values when changing the weighting factors of f_1 and f_3 by approximately 53 % and 42.6 %, respectively. After analyzing six cases, the results show a strong contradiction between the f_1 and f_3 objectives. Similarly, the results imply an inverse relationship between f_1 and f_2. f_2 and f_3 tended to increase or decrease together simultaneously. Therefore, improving one objective might involve trade-offs with the other objectives, especially between f_1 and f_3.

4.2.3. Comparison with other multi-objective method

In general, the mathematical model of the proposed IEH can be solved by the ε-constraint method, which is well-known and has been applied to various multi-objective optimization (MOP) problems. The ε-constraint method is used to reformulate MOP by maintaining only one objective and limiting the other objective to specified values. The comprehensive mathematical of the ε-constraint method can be found in [52]. In this section, the proposed NWS is compared with the ε-constraint to solve the MOP of the IEH under study. The optimal cases considered the operating costs as the primary objective function, followed by carbon emissions and EEI ($\omega_1 = 3/6$, $\omega_2 = 2/6$, and $\omega_3 = 1/6$). For ε-constraint, ten grid points are selected for each objective function, as with the default number of the grids given in the GAMS Model library [66]. The results of MOP methods for the considered cases are presented in Table 8.

The optimal solutions of the proposed NWS dominate those achieved by the ε-constraint in two objective functions for the case under study.
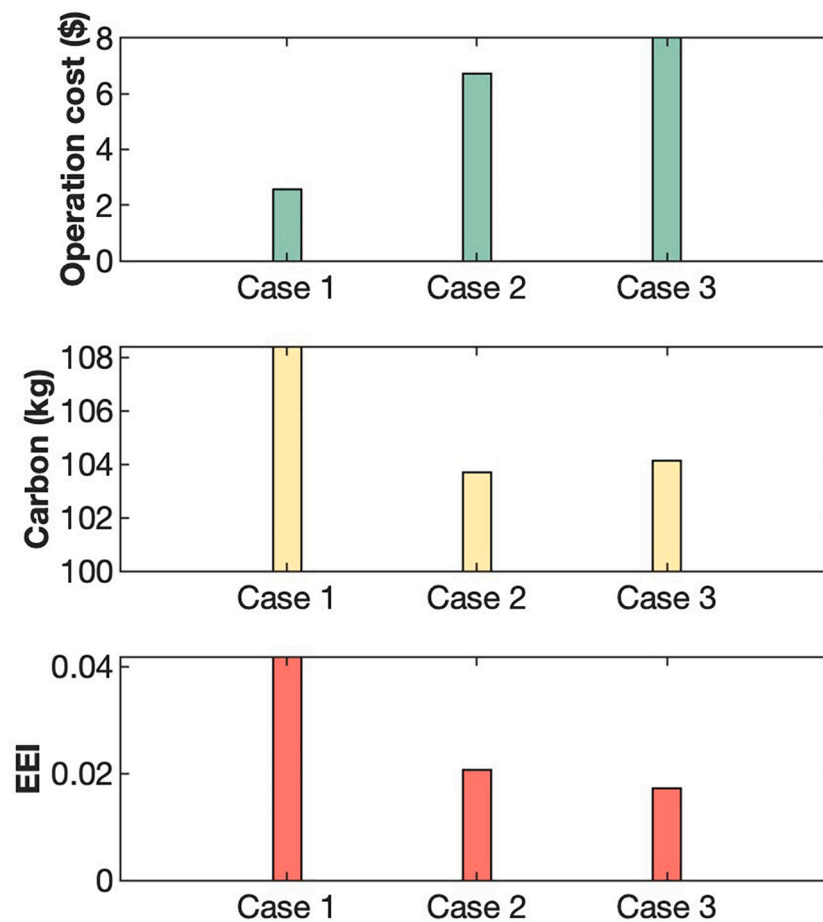
Fig. 11. Results of each objective function in case of for single-objective optimization.

Carbon emission and EEI are reduced by 0.57 % and 3,17 %, respectively, while operation cost increases by 1.46 % compared to the ε-constraint. Another highlight is that NWS has a lower computation time with better performance. For ε-constraint, ten grid points are selected for each objective function, resulting in $10 \times 10 = 100$ subproblems to be solved, which requires more computational time.

4.2.4. Effects of the BESS and HSS on the biomass electrolyzer operation

The effective transition to eco-friendly energy concepts relies heavily on stationary energy storage systems. These systems enable the efficient utilization of the varying outputs from renewable energy sources. Hydrogen technologies, such as fuel cells and electrolysis systems, are also gaining significance. They complement battery storage systems and are particularly valuable for long-term sustainable energy storage. This subsection evaluates the impact of battery and hydrogen storage systems on IEH operation. The scenarios are as follows:

- S1- RES-connected biomass electrolyzer stack: RES and grid supply the energy for the biomass electrolyzer; ESS is not utilized.
- S2- RES/BESS-connected biomass electrolyzer stack: When the RES generation exceeds demand, the excess electricity produced by the RES is stored in the BESS.
- S3- RES/HSS-connected biomass electrolyzer stack: Similar to S2, but the excess energy is stored as hydrogen energy in the HSS instead of the BESS.
- S4- RES/BESS/HSS-connected biomass electrolyzer stack: RES provides power to the grid-connected electrolyzer, and the BESS and HSS are used concurrently. Thus, a portion of the electricity is sold to the market or stored in the BESS. The hydrogen produced is used to meet demand, and the remainder is stored in the HSS.

Table 9 shows the results of objectives in simulation cases to evaluate the impact of ESS on IEH performance. Different combinations of BESS and HSS are used to analyze their impact on IEH operation. The effect of multiple storage systems on IEH operations depends on various parameters, including the IEH model and components, energy carrier pricing profiles, demand profiles, charge/discharge/storage efficiencies, storage capacity, and so on. In the first scenario, the operating cost of IEH without ESS is $9.4421. When only BESS, only HSS, and both BESS and HSS are used, the operating costs are reduced by 56.38 %, 67.89 %, and 71.78 %, respectively. Meanwhile, the remaining two objective functions are also significantly reduced. In the second scenario, the carbon emission and EEI are reduced by 69.32 % and 84.38 %, respectively. In the scenario with only HSS, the result of f_2 and f_3 decrease by 62.48 % and 75.15 %, respectively while, in the case of BESS and HSS, f_2 and f_3 were reduced by 79 % and 95.56 %, respectively. As a result, by integrating the HSS into the ESS, the model significantly reduces IEH operation costs by 35.29 %, reduces carbon emission by 33.37 %, and improves EEI by 71.6 % compared with only using BESS.

Table 10 compares the average carbon coefficients of CO_2 emissions per kilogram of hydrogen produced. The table shows the carbon intensity of biomass electrolysis, which is currently the primary method used to produce green hydrogen. The results demonstrated that S1 had the highest CO2 intensity coefficient. However, with the addition of ESS, the coefficient decreased significantly, with the most significant reductions observed in S2, S3 and S4. S4 reduced approximately 6.5627 kg of CO_2 compared with S1 without an ESS. S3 and S4 show promising results, with only a 0.5689 kg emission difference between these scenarios. The technical parameters of the biomass electrolyzer are shown in Fig. 18. For S3 and S4, the electrolyzer is not used at intervals of 1 h–3 h when hydrogen demand is low, and the hydrogen stored in HSS is used
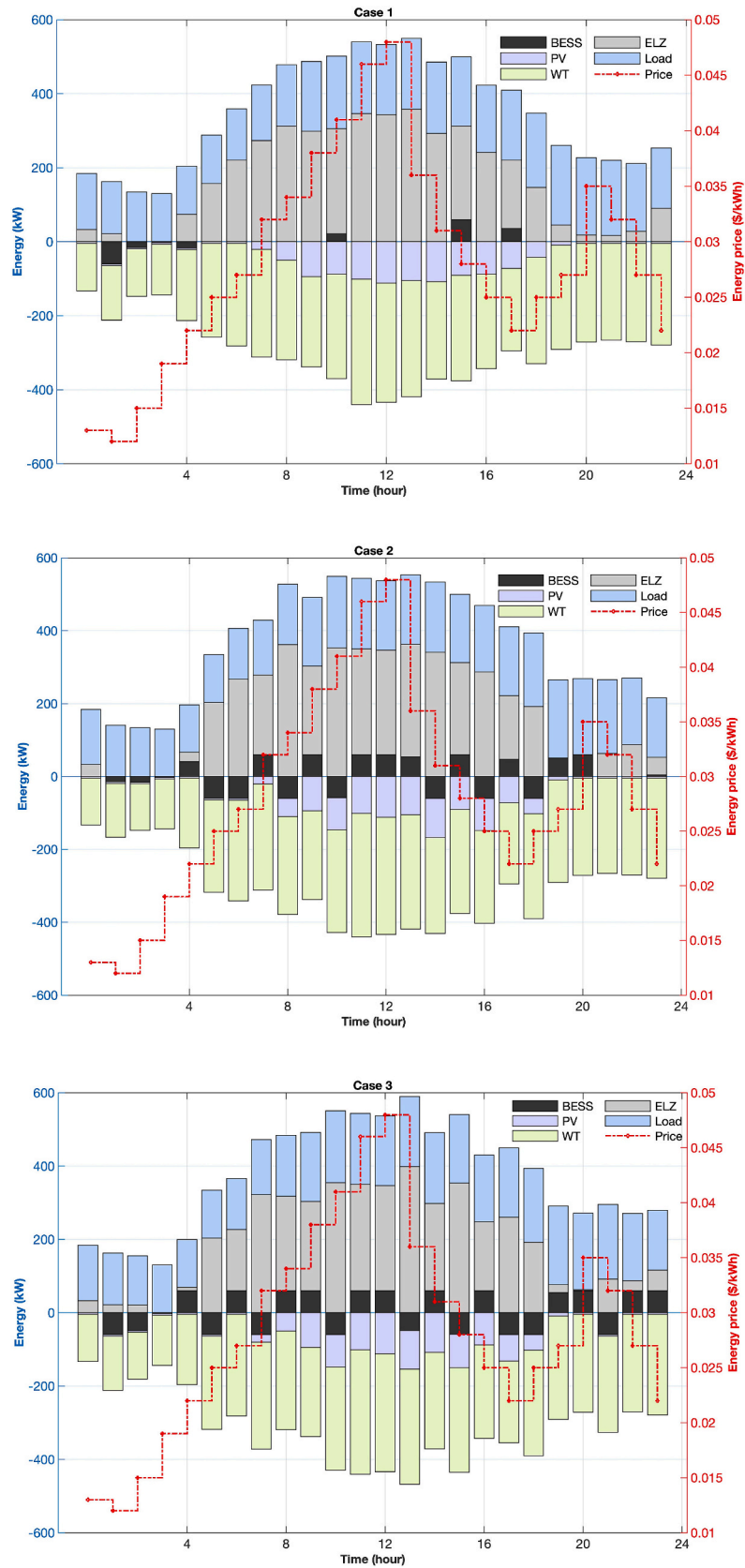
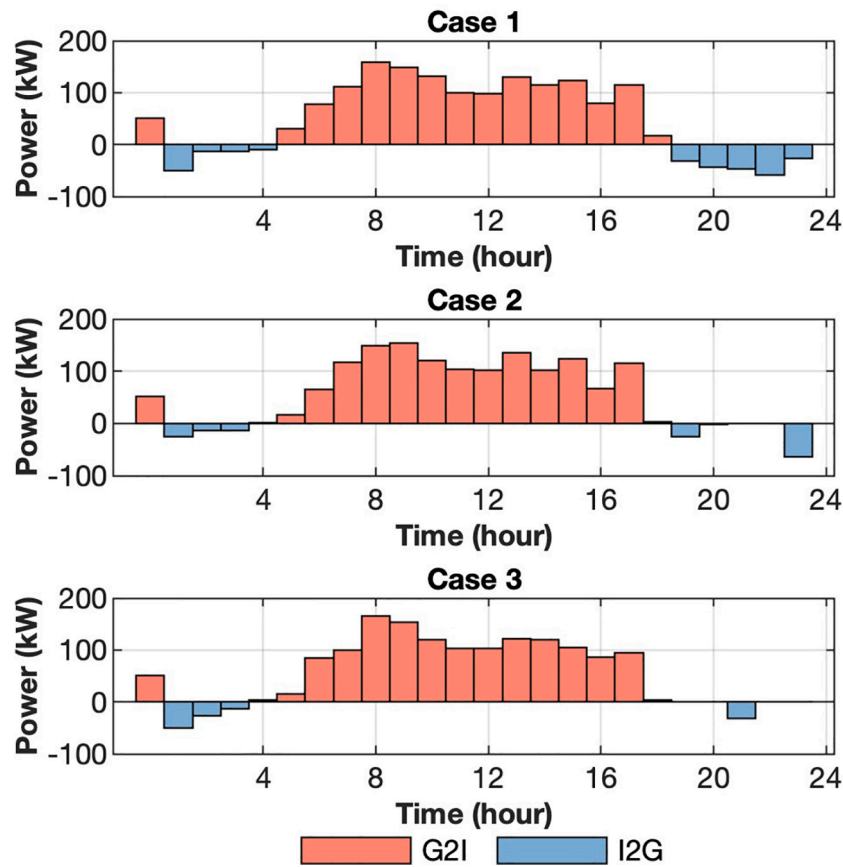**Fig. 12.** Scheduling profile for each objective optimization problem.

Fig. 13. Electrical energy transactions between IEH and the grid.
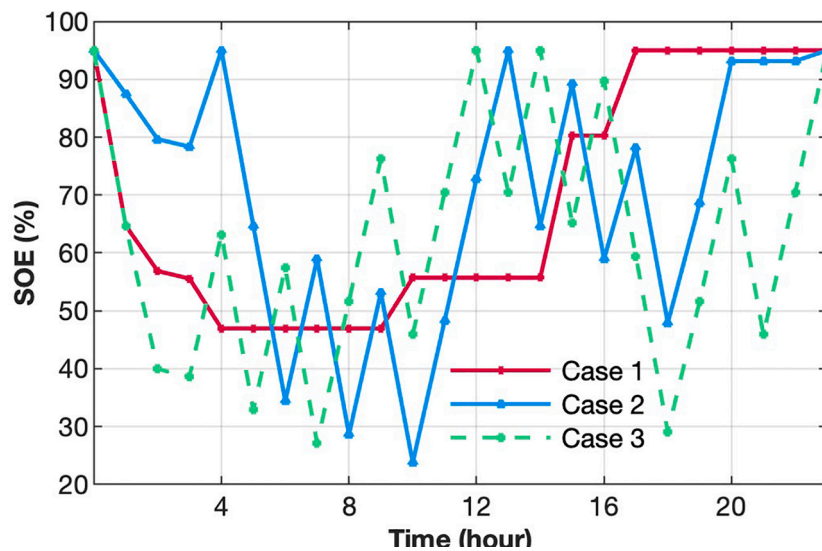

Fig. 14. SOC of the BESS for each objective.

to reduce the operation costs of the electrolyzer. However, from hours 21 to 23 h, the electrolysis current exhibits continuous and dramatic changes when the load demand is low. In such situations, the electrolyzer increases hydrogen production for storage by utilizing the excess RES energy, as depicted in Fig. 19. The simulation results indicate that the ESS provides high operational flexibility for IEH to handle redundant or deficient RES generation, similar to hydrogen.

4.3. Optimization of IEH considering uncertainties

The proposed IGDT-NWS model for the IEH under study has 96 uncertain data points, including electricity and hydrogen demand, RES production, and energy prices. To achieve the desired objective functions while maintaining the operation cost of IEH within acceptable limits, it is crucial to study these uncertainties and assess their impact on the operating costs and future planning. The operator's perspective plays a vital role in optimal decision-making. Hence, this study considers
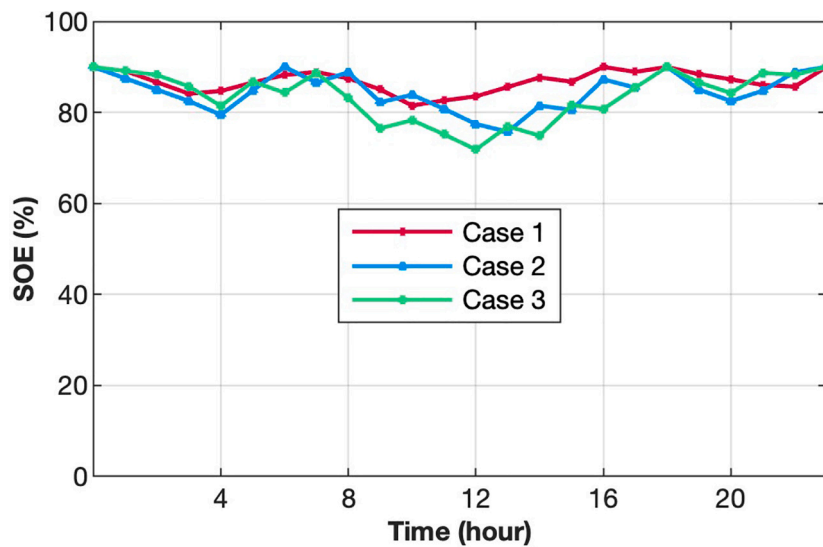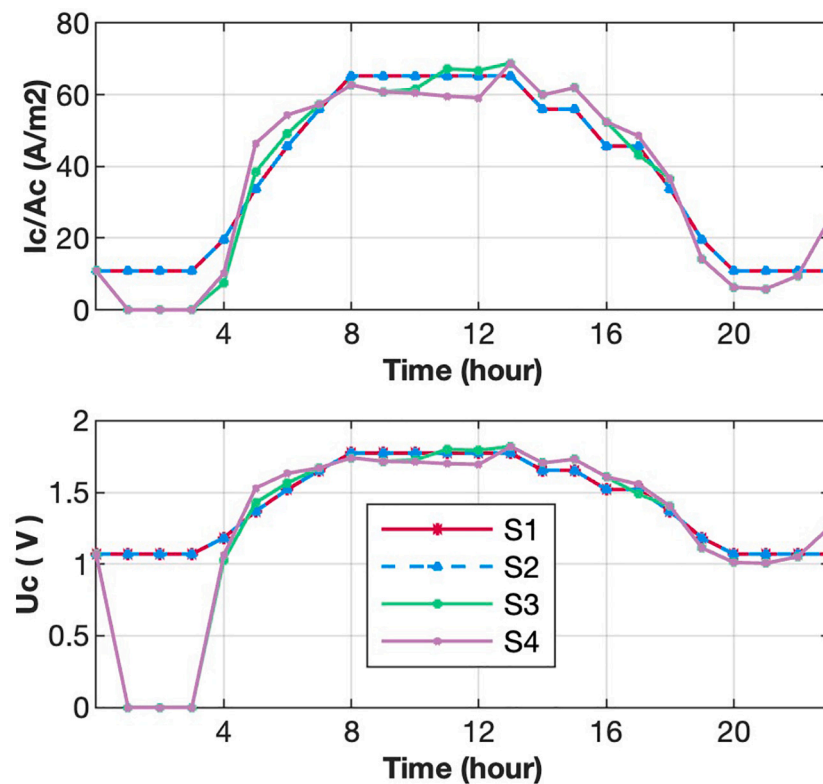
Fig. 15. SOC of HSS for each objective.

Fig. 16. Operation technical parameters of the biomass electrolyzer with three cases.

both the risk-averse and risk-seeking decision-making strategies of the IGDT approach. The optimal cases considered the operating costs as the primary objective function, followed by carbon emissions and EEI ($\omega_1 = 3/6$, $\omega_2 = 2/6$, and $\omega_3 = 1/6$).

4.3.1. Risk-Averse Strategy

The risk-averse (RA) strategy is an IGDT model that considers the uncertainty of input data. It aims to maximize the uncertainty or confidence range to ensure that any deviation from the uncertainty in the confidence set does not exceed the critical value of the objective function. For the operating cost objective function, the RA strategy does not focus on minimizing operating costs of the IEH but on maximizing the sustainability range. This ensures that the worst-case operational costs do not exceed a certain threshold, even if this implies increasing the IEH operating costs for better durability and protection from potential adverse deviations. While balancing load and generation, operators must consider the risks of increased demand and reduced generation resources in their RA strategy. The IEH scheduling subsection considers uncertainties, such as electric and hydrogen demands, RES output, and the price of energy transactions with the power grid. The impact of each uncertain variable on the values of the objectives, decision variables, and scheduling operations from the RA perspective was investigated.
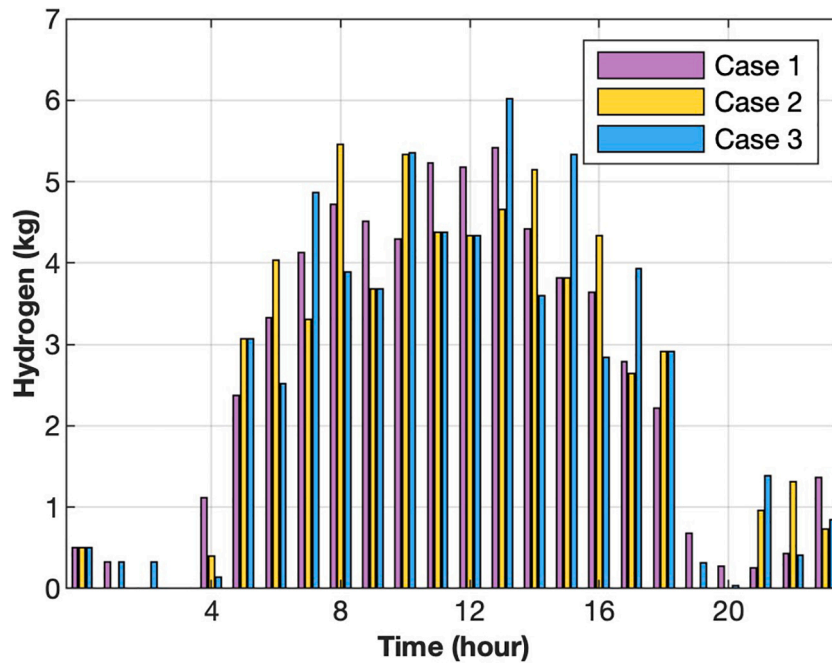
Fig. 17. Green hydrogen production of IEH with three cases.

Table 7
The optimal solutions of multi-objective under different cases.

Case	Weighting factors value			Objective value		
	ω_1	ω_2	ω_3	f_1	f_2	f_3
1	3/6	2/6	1/6	2.6647	106.406	0.0366
2	3/6	1/6	2/6	2.6773	106.3617	0.0364
3	2/6	3/6	1/6	2.7836	106.1342	0.0351
4	1/6	3/6	2/6	5.5452	103.7411	0.0215
5	2/6	1/6	3/6	3.1409	105.778	0.032
6	1/6	2/6	3/6	5.6818	103.829	0.021

Table 8
Comparison results between the proposed method and ε-constraint method.

Method	Operation cost	Carbon emission	EEI	Computational time (s)
ε-constraint	2.6263	107.0167	0.0378	90.62
Proposed	2.6647	106.406	0.0366	38.26

Table 9
The optimal solutions of multi-objective under different scenarios.

Scenarios	f_1	f_2	f_3
Scenarios 1: Without ESS	9.4421	506.687	0.8251
Scenarios 2: Only BESS	4.1182	155.428	0.1289
Scenarios 3: Only HSS	3.032	190.1333	0.205
Scenarios 4: BESS and HSS	2.6647	106.406	0.0366

Table 10
Ratio of CO_2 per hydrogen produced.

Scenarios	$\dfrac{kg_{CO_2}}{kg_{H_2}}$
S1: Without ESS	8.3063
S2: Only BESS	2.548
S3: Only HSS	3.1169
S4: BESS and HSS	1.7436

A) *IEH scheduling considering single uncertainty:* The uncertainty of electric and hydrogen demands, output of PV and WT, and the electricity price are considered separately. In this regard, each uncertain variable is evaluated from the risk-averse perspective to the IEH operation cost. Table 11 and Fig. 20 indicate the robustness horizon for each uncertain data for different critical operation cost deviation factors. The simulation results show that the deviations in electricity demand, hydrogen demand, and output of WT are crucial in the operation of the IEH. For instance, the robustness horizon of the electric demand is 0.0785 if the critical cost deviation factor β is 0.10. It means the IEH operation cost will be at most 10 % higher than the nominal operation cost if the electricity demand deviates within a 7.85 % band concentrated at their forecasted values. According to the results in Table 11, for the critical operation cost of \$2.9312, the maximum robustness horizon considering the uncertainties of electricity demand, hydrogen demand, PV and WT output, and the electricity price are 0.0785, 0.0552, 0.2555, 0.0495, and 0.2529, respectively. Therefore, operating costs do not exceed the critical cost when electricity demand, hydrogen demand, the output of PV and WT, and the electricity price fluctuate from forecast values within 7.85 %, 5.52 %, 25.55 %, 4.95 %, and 25.29 %, respectively. Similarly, the other cases can be considered.

B) *IEH scheduling considering all uncertainties:* In this case, the uncertainties of electricity demand, hydrogen demand, the output of RES, and the electricity price are simultaneously considered. Therefore, IEH scheduling with all uncertainties aims to maximize the robustness horizon and not to exceed critical operation costs. Considering all uncertainties with α^{total} are equal to $\alpha^{load} + \alpha^e + \alpha^{PV} + \alpha^{WT} + \alpha^H$, the operation scheduling for deviation factor $\beta = 0.10$ is done. According to Table 12, the total robustness horizon α^{total} is equal to 0.2556. The operation cost of the IEH is guaranteed not to be higher than \$2.9312 if electricity demand, hydrogen demand, the output of PV and WT, and the electricity price do not deviate from the 5 %, 1.24 %, 10 %, 7.06 %, and 17.2 % with forecasted value, respectively.
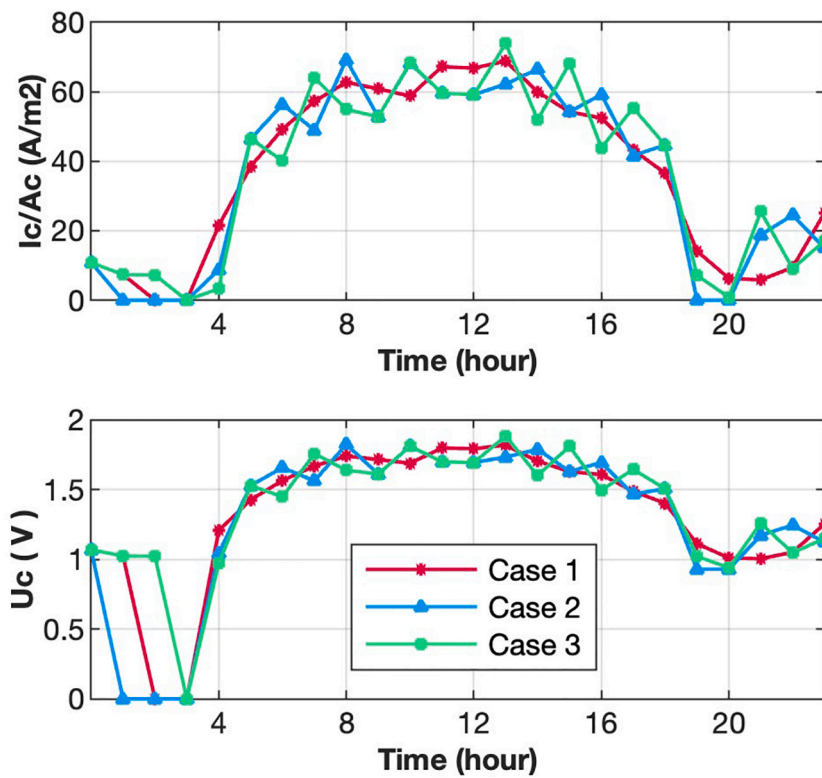
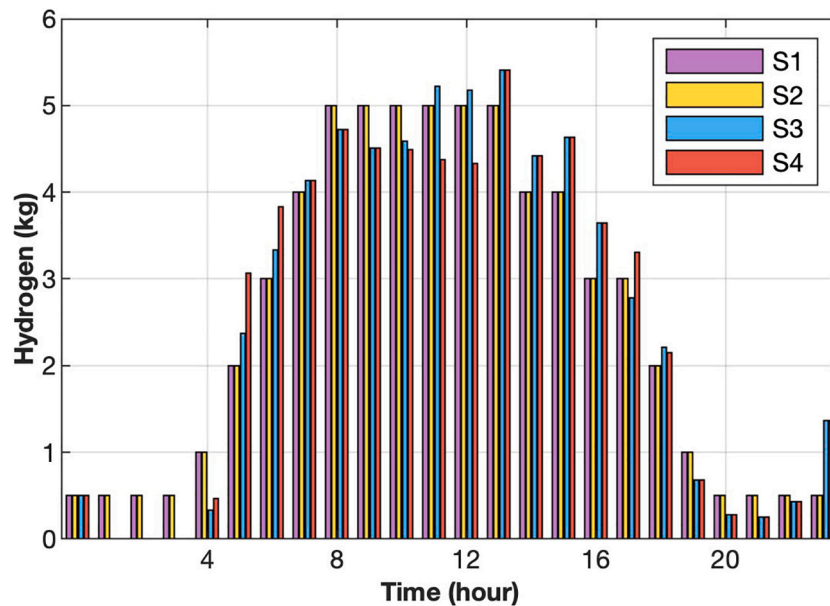**Fig. 18.** Technical variables of electrolyzer cells.

Fig. 19. The hydrogen produce rate of each scenario.

4.3.2. Risk-Seeker Strategy

This section presents the computational cases of the risk-seeking (RS) model. Decisions on scheduling activities in the IEH are made from the perspective of an optimistic decision-maker. The resulting values of the objective functions, such as the amount of electricity traded with the grid and the amount of hydrogen produced, are determined based on the outlook of an optimistic decision-maker seeking the risk and opportunity scope of the factors. In this model, the objective is not to minimize operating costs but rather to identify the minimum required deviation of the input data into various uncertainties to achieve the target operating costs.

A) *IEH scheduling considering single uncertainty:* The uncertainty of electric and hydrogen demands, PV and wind power generation, and the price of electricity purchased from the power grid are considered separately. In this regard, each uncertain variable is evaluated from an optimistic risk-seeker operator. Table 13 *indicates the* opportunity horizon for each uncertain data for different target operation cost deviation factors ρ. According to the Table 13, for the target operation cost of $2.3982 or deviation factor $\rho = 0.1$, the minimum opportunity horizon considering the uncertainties of electricity demand, hydrogen demand, PV and

Table 11
Compared effect of deviation factors β on objective values and decision variables.

β	Critical operation cost ($)	α^{load}	α^{e}	α^{PV}	α^{WT}	α^{H}
0.01	2.6913	0.0466	0.0208	0.1479	0.0291	0.032
0.03	2.7446	0.0537	0.0624	0.1718	0.0338	0.0371
0.05	2.7979	0.0608	0.1042	0.1957	0.0383	0.0423
0.10	2.9312	0.0785	0.2529	0.2555	0.0495	0.0552
0.15	3.0644	0.0962	0.2564	0.315	0.0606	0.0681
0.20	3.1976	0.1136	0.3532	0.3737	0.0717	0.081
0.25	3.3309	0.1310	0.4328	0.4325	0.0827	0.0937
0.30	3.4641	0.1479	0.4535	0.4914	0.0936	0.1065
0.40	3.7306	0.1793	0.585	0.609	0.1153	0.1319
0.50	3.9971	0.2107	0.7373	0.7265	0.1355	0.1573

WT output, and the electricity price are 0.4834, 0.1483, 0.2555, 0.1512, and 0.3291, respectively. Considering a target cost deviation factor of 0.10 means that the decision-maker obtains decision variables and opportunity horizons to achieve an operation cost 10 % lower than the nominal cost. The results show that operating costs can satisfy the target cost when electricity demand, hydrogen demand, the output of PV and WT, and the electricity price fluctuate from forecast values within 48.34 %, 14.83 %, 25.55 %, 15.12 %, and 32.91 %, respectively.

B) *IEH scheduling considering all uncertainties:* Table 14 indicates the total opportunity horizon for $\rho = 0.10$ of target operation cost. According to Table 14, the total opportunity horizon α^{total} is equal to 0.2569. The operation cost of the IEH is guaranteed not to be higher than \$2.3982 if the output of WT matches the predicted value. Meanwhile, electricity load, hydrogen demand, the output of PV, and the electricity price are within the range of 4.83 %, 5.86 %, 10 %, and 5 % of forecasted values, respectively.

4.4. Comparison of decision variables for without-uncertainties, risk-averse, risk-seeking decision-making, robust optimization

In this section, considering energy price uncertainty from the transaction with the power grid, a comparison of optimal objectives and

Table 12
Total robustness horizon for 0.10 deviation factor of critical operation cost.

β	α^{total}	α^{load}	α^{e}	α^{PV}	α^{WT}	α^{H}
0.10	0.2556	0.05	0.1720	0.1	0.0706	0.0124

Table 13
Compared effect of deviation factors ρ on objective values and decision variables.

ρ	Target operation cost ($)	α^{load}	α^{e}	α^{PV}	α^{WT}	α^{H}
0.01	2.6381	0.3307	0.1565	0.1479	0.1246	0.1255
0.03	2.5848	0.3646	0.1941	0.1718	0.1305	0.1305
0.05	2.5315	0.3986	0.2327	0.1957	0.1364	0.1356
0.10	2.3982	0.4834	0.3291	0.2555	0.1512	0.1483
0.15	2.265	NA	0.4255	0.315	0.1659	0.1610
0.20	2.1318	NA	0.522	0.3737	0.1806	0.1737
0.25	1.9985	NA	0.6184	0.4325	0.1954	0.1864
0.30	1.8653	NA	0.7149	0.4914	0.2164	0.1992
0.40	1.5988	NA	NA	0.609	0.261	0.2252
0.50	1.3324	NA	NA	0.7265	0.3057	0.2512

Table 14
Total opportunity horizon for 0.10 deviation factor of target operation cost.

ρ	α^{total}	α^{load}	α^{e}	α^{PV}	α^{WT}	α^{H}
0.10	0.2569	0.0483	0.05	0.1	0	0.0586

the impact of uncertainty on IEH operation for without-uncertainty, RA, RS, and robust optimization is presented. The robust optimization (RO) method provides valuable results in scenarios characterized by high uncertainty and lacking input data regarding random factors. RO ensures the issue has been resolved against the uncertainty parameters in one scenario called "the worst-case scenario" and indicates the decision-conservation level for the decision-maker. A comprehensive mathematical of RO has been described in [6,39]. The results are presented in Tables 15–16 and Fig. 21.
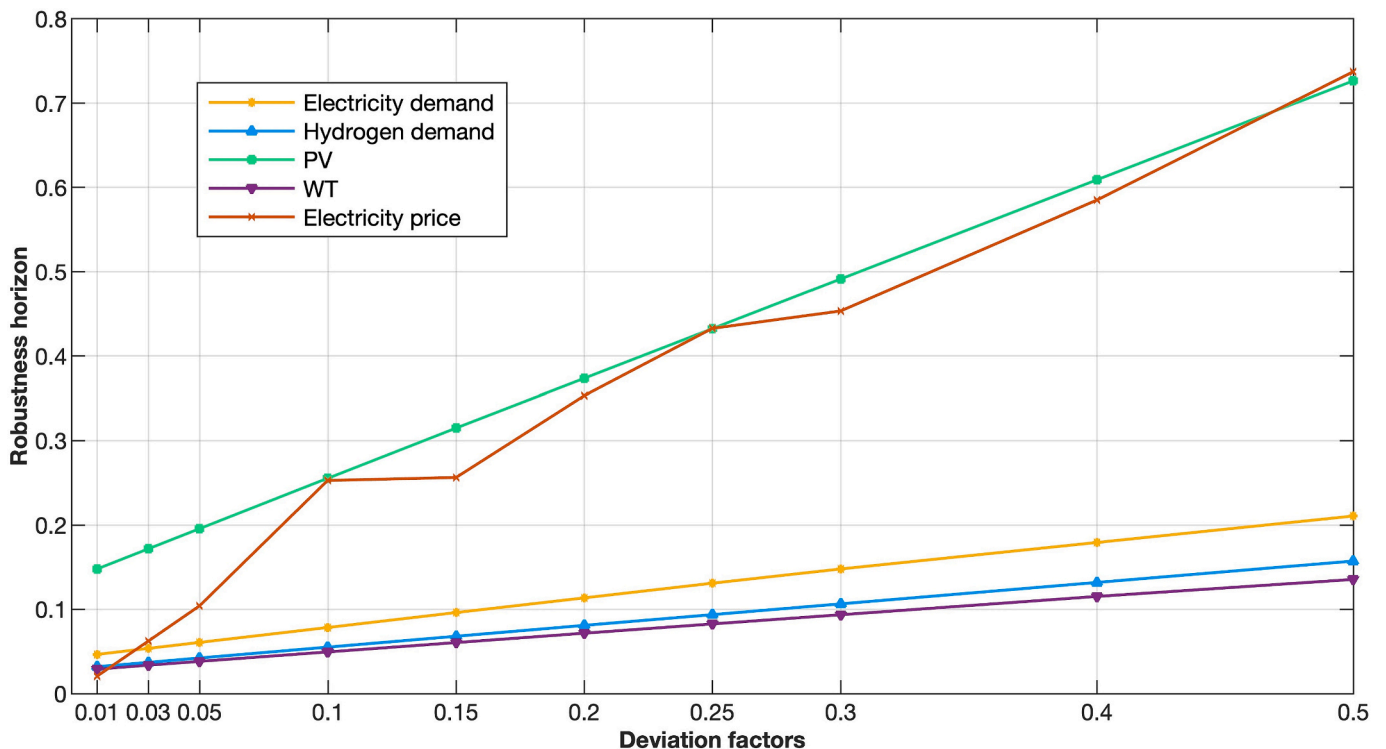

Fig. 20. Acceptable deviation from different input data guarantees critical operation cost.

Table 15
Compared objective values for each case.

Case	f_1	f_2	f_3
Case 1: Without uncertainties	2.6647	106.406	0.0366
Case 2: Risk-Averse Strategy ($\beta = 0.1$)	2.9311	117.0466	0
Case 3: Risk-Seeker Strategy ($\rho = 0.1$)	2.3982	90.4856	0.0421
Case 4: Robust optimization (RO)	6.9922	117.0466	0.0292

Fig. 21 and Table 16 compare the decision variables in the transaction energy for the without-uncertainties, risk-averse, risk-seeking, and robust optimization (RO). The results show that the RO strategy always considers buying from the grid in the worst-case scenario, where the RES output is insufficient to meet the load demand. Therefore, the amount of electricity purchased from the grid with the RO method is the highest. Meanwhile, the RS method, with an optimistic view of the decision-maker, does not buy electricity from the grid most of the time and has superior export to the grid in the case of not considering uncertainty, RA, and RO, especially during periods of low load demand compared to the RES output (1–4 h) and (19–23 h). Across most hours, hourly energy buying by the RA strategy and RO tends to have higher costs for buying electricity, whereas the RS strategy reduces 22.69 % and 28.4 %, respectively. This result is because the RS considers the possibility of changing the uncertainty output of the RESs in a favorable direction within the allowed confidence range to ensure a total supply of load needs without buying electricity from the grid. The IEH operator increases the electricity exported to the power grid and reduces the electricity purchased from the grid. In contrast, in RA decision-making, the IEH purchases restrictions on electricity from the power grid to decrease the impact of the price uncertainty of electricity purchased from the power grid. As shown in Table 15, the cost of the RA increases by 9.1 %, whereas the RS reduces the cost by 10 % compared to the case where uncertainty is not considered. For RO, the operator has a much more pessimistic view of uncertain factors, making the operating costs very high compared to other cases.

5. Conclusions

This paper proposes a comprehensive IEH model that fully utilizes solar PV and wind turbine power generation to produce green hydrogen using a biomass electrolyzer with BESS and HSS. The proposed IEH was developed as a multi-objective problem with three objective functions: operational cost, carbon emissions, and EEI objectives. The NWS was proposed to solve the multi-objective problems in various simulation cases. Scheduling of the IEH for producing green hydrogen was performed assuming no uncertainty, RA, RS, and RO. This study investigated the impacts of the risk and deviation factors of critical and target costs on IEH operational costs. The IGDT method is a risk-aware method that handles uncertainties in electric and hydrogen demands, RES output, and energy prices. In addition, this study compared the results of the optimal IEH operation with and without uncertainties.

In this study, we also examined the impact of ESS on IEH operations. Multiple variables, such as the IEH model, energy pricing, demand profiles, efficiencies, and storage capacities, influence the impact of ESS. The results showed that energy storage systems significantly affected the operation of IEHs, leading to substantial cost reductions and improvements in other objective functions. The BESS and HSS provide significant cost reductions and other operational improvements, indicating their economic viability. Using only the BESS, only HSS, and both BESS and HSS can reduce the operation costs by 56.38 %, 67.89 %, and 71.78 %, respectively. The combination of BESS and HSS offers the most environmentally friendly solution, reducing carbon emissions by up to 79 % and the energy export index EEI by 95.56 %. This study suggests that IEHs with multiple types of ESS are more flexible and efficient in operations and can adapt to various energy prices and demand profiles. The results show that by integrating the HSS into the ESS, the model significantly reduces IEH operation costs by 35.29 %, reduces carbon emission by 33.37 %, and improves EEI by 71.6 % compared with only using BESS. In future work, it would be interesting to investigate how these benefits scale with the IEH's size and examine the trade-offs between initial investment in the ESS and long-term operational cost savings.
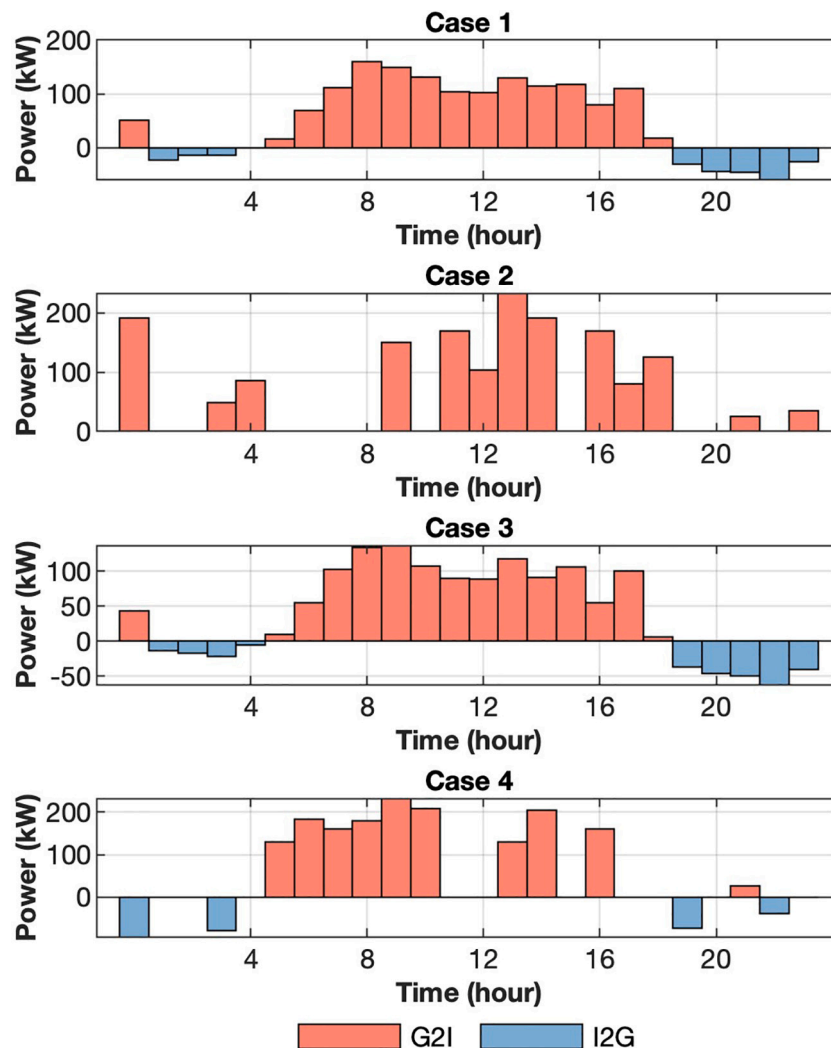
Table 16
Compare objective values for each case.

Hour	Without uncertainties		Risk-Averse Strategy ($\beta = 0.1$)		Risk-Seeker Strategy ($\rho = 0.1$)		Robust optimization	
	G2I (kW)	I2G (kW)	G2I (kW)	I2G (kW)	G2I (kW)	I2G (kW)	G2I (kW)	I2G (kW)
0	50.9	0	191.65	0	43.1867	0	53.742	0
1	0	23.0866	0	0	0	14.4178	0	30.2549
2	0	13.7092	0	0	0	17.2244	60.9827	0
3	0	13.7718	48.7699	0	0	22.6059	0	26.8412
4	0	0	85.2129	0	0	5.3326	3.6717	0
5	15.9314	0	0	0	9.8264	0	20.8994	0
6	68.4048	0	0	0	55.3918	0	86.2184	0
7	112.0250	0	0	0	102.9233	0	118.5875	0
8	159.4698	0	0	0	134.1188	0	154.0078	0
9	148.7393	0	149.8685	0	137.0301	0	156.0579	0
10	130.4704	0	0	0	107.3920	0	125.3023	0
11	103.9112	0	170.3684	0	89.8189	0	106.193	0
12	102.7340	0	103.5471	0	89.0184	0	95.0405	0
13	130.3456	0	233.579	0	117.8822	0	125.4174	0
14	114.4089	0	191.813	0	90.6582	0	122.6509	0
15	117.7388	0	0	0	106.1053	0	126.7262	0
16	80.2854	0	169.1665	0	54.8891	0	89.3365	0
17	110.0314	0	80.2559	0	100.4942	0	100.8379	0
18	17.6318	0	125.2503	0	5.3954	0	26.13709	0
19	0	31.0354	0	0	0	36.6226	0	40.3744
20	0	44.0184	0	0	0	46.9267	0	51.8337
21	0	46.4708	24.9983	0	0	49.5684	0	23.3228
22	0	58.8239	0	0	0	62.2322	0	32.668
23	0	25.9514	34.8510	0	0	40.8156	37.522	0
Total	1463.0281	256.8676	1609.3309	0	1244.1309	295.7463	1737.7524	0

Fig. 21. Electricity trading for each case.

When comparing decision variables in scenarios without uncertainties as well as in risk-averse (RA), risk-seeking (RS), and robust decision-making, it was found that the IEH operator purchases less electricity from the power grid when making risk-seeking decisions to hedge against the risk of electricity price and demand deviations. On the other hand, in the RA strategy and RO, the IEH buys more electricity from the power grid than without uncertainty, and ignoring the price uncertainty of electricity purchased from the power grid to decrease its operation cost and meet demand can increase significantly. The two strategies of the IGDT approach result in a planning schedule that is more uncertainty-aware and more effective in terms of economics. The planning obtained for IEH with RA strategy is robust against the maximum prediction error of electricity demand, hydrogen demand, the output of PV and WT, and the electricity price of 5 %, 1.24 %, 10 %, 7.06 %, and 17.2 %, respectively. With the RS strategy, our proposed method can optimistically reduce operation cost by 10 % with the output of WT matches the predicted value. Meanwhile, electricity load, hydrogen demand, the output of PV, and the electricity price are within the range of 4.83 %, 5.86 %, 10 %, and 5 % of forecasted values, respectively. The normalized weighted-sum approaches to solve multi-objective problems resulted in compromised and efficient solutions in which the objectives were close to the ideal values. The IEH operators can consider multiple weighting factor options to satisfy different operating requirements.

It should be noted that each subsystem has some impact on the functioning of the IEH, and its impact can be increased or decreased depending on the underlying structure of the IEH. Although the conclusions drawn in this study are based on the schematic of the proposed IEH shown in Fig. 2, integration of other subsystems, such as thermal storage systems, can significantly impact the overall performance of the IEH. Therefore, any changes to the structure of the proposed IEH model (such as adding another type of energy storage) would be followed by thoroughly detailed analysis for the new architecture, which is one of our future works. Furthermore, developing methods that integrate machine learning algorithms into predictive modeling and decision-making in the IEH could be beneficial. Deploying advanced machine learning and data analytics techniques can provide more accurate predictions of energy production, consumption, and storage behavior, thus enhancing IEH operation efficiency.

CRediT authorship contribution statement

Pham Van Phu: Writing – original draft, Visualization, Validation, Methodology, Investigation, Conceptualization. **Truong Hoang Bao Huy:** Visualization, Validation, Investigation, Formal analysis. **Seong-keun Park:** Writing – review & editing, Supervision, Methodology, Formal analysis. **Daehee Kim:** Writing – review & editing, Supervision, Methodology, Funding acquisition, Formal analysis, Conceptualization.

Declaration of competing interest

The authors declare that they have no known competing financial interests or personal relationships that could have appeared to influence the work reported in this paper.

Data availability

Data will be made available on request.

Acknowledgments

References

[1] T. Hibino, K. Kobayashi, M. Ito, Q. Ma, M. Nagao, M. Fukui, S. Teranishi, Efficient hydrogen production by direct electrolysis of waste biomass at intermediate tempera- tures, ACS Sustain. Chem. Eng. 6 (7) (2018) 9360–9368.

[2] M. Nasir, A.R. Jordehi, S.A.A. Matin, V.S. Tabar, M. Tostado-Véliz, S.A. Mansouri, Optimal operation of energy hubs including parking lots for hydrogen vehicles and responsive demands, J. Energy Storage 50 (104630) (2022).

[3] E. Akbari, S.F.M. Shabestari, S. Pirouzi, M. Jadidoleslam, Network flexibility regulation by renewable energy hubs using flexibility pricing-based energy management, Renew. Energy 206 (2023) 295–308.

[4] M. Mohammadi, Y. Noorollahi, B. Mohammadi-ivatloo, H. Yousefi, Energy hub: from a model to a concept – a review, Renew. Sust. Energ. Rev. 80 (2017) 1512–1527.

[5] Z. Qu, C. Xu, F. Yang, F. Ling, S. Pirouzi, Market clearing price-based energy management of grid-connected renewable energy hubs including flexible sources according to thermal, hydrogen, and compressed air storage systems, J. Energy Storage 69 (107981) (2023).

[6] G. Piltan, S. Pirouzi, A. Azarhooshang, A.R. Jordehi, A. Paeizi, M. Ghadamyari, Storage-integrated virtual power plants for resiliency enhancement of smart distribution systems, J. Energy Storage 55 (105563) (2022).

[7] J. Wang, H. Zhong, Z. Yang, M. Wang, D.M. Kammen, Z. Liu, Z. Ma, Q. Xia, C. Kang, Exploring the trade-offs between electric heating policy and carbon mitigation in China, Nat. Commun. 11 (6054) (2020).

[8] E. Papadis, G. Tsatsaronis, Challenges in the decarbonization of the energy sector, Energy 205 (118025) (2020).

[9] T. Lepage, M. Kammoun, Q. Schmetz, A. Richel, Biomass-to-hydrogen: a review of main routes production, processes evaluation and techno-economical assessment, Biomass Bioenergy 144 (105920) (2021).

[10] L. An, T.S. Zhao, Z.H. Chai, P. Tan, L. Zeng, Mathematical modeling of an anion-exchange membrane water electrolyzer for hydrogen production, Int. J. Hydrog. Energy 39 (35) (2014).

[11] T.N.A. Tran, T.M. Khoi, N.M. Phuoc, H.B. Jung, Y. Cho, A review of recent advances in electrode materials and applications for flow-electrode desalination systems, Desalination 541 (116037) (2022).

[12] P. Xiao, W. Hu, X. Xu, W. Liu, Q. Huang, Z. Chen, Optimal operation of a wind-electrolytic hydrogen storage system in the electricity/hydrogen markets, Int. J. Hydrog. Energy 45 (46) (2020) 24412–24423.

[13] A. Buttler, H. Spliethoff, Current status of water electrolysis for energy storage, grid balancing and sector coupling via power-to-gas and power-to-liquids: a review author links open overlay panel, Renew. Sust. Energ. Rev. 82 (2018) 2440–2454.

[14] Z. Zeb, Y. Huang, L. Chen, W. Zhou, M. Liao, Y. Jiang, H. Li, L. Wang, L. Wang, H. Wang, T. Wei, D. Zang, Z. Fan, Y. Wei, Comprehensive overview of polyoxometa- lates for electrocatalytic hydrogen evolution reaction, Coord. Chem. Rev. 482 (215058) (2023).

[15] I.A. Gondal, S.A. Masood, R. Khan, Green hydrogen production potential for developing a hydrogen economy in Pakistan, Int. J. Hydrog. Energy 43 (12) (2018) 6011–6039.

[16] Y. Kalinci, A. Hepbasli, I. Dincer, Biomass-based hydrogen production: a review and analysis, Int. J. Hydrog. Energy 34 (2009).

[17] H. Oh, Y. Choi, C. Shin, T.V.T. Nguyen, Y. Han, H. Kim, Y.H. Kim, J.-W. Lee, J.-W. Jang, J. Ryu, Phosphomolybdic acid as a catalyst for oxidative valorization of biomass and its application as an alternative electron source, Am. Chem. Soc. 10 (3) (2020) 2060–2068.

[18] J. Yao, M. Kraussler, F. Benedikt, H. Hofbauer, Techno-economic assessment of hydrogen production based on dual fluidized bed biomass steam gasification, biogas steam reforming, and alkaline water electrolysis processes, Energy Convers. Manag. 145 (2017) 278–292.

[20] P. Mancarella, MES (multi-energy systems): an overview of concepts and evaluation models, Energy 65 (2014) 1–17.

[21] E. Alizad, H. Rastegar, F. Hasanzad, Dynamic planning of power-to-gas integrated energy hub considering demand response programs and future market conditions, Int. J. Electr. Power Energy Syst. 143 (108503) (2022).

[22] X. Xu, W. Hu, D. Cao, Q. Huang, W. Liu, M.Z. Jacobson, Z. Chen, Optimal operational strategy for an offgrid hybrid hydrogen/electricity refueling station powered by solar photovoltaics, J. Power Sources 451 (227810) (2020).

[23] I. Sorrenti, Y. Zheng, A. Singlitico, S. You, Low-carbon and cost-efficient hydrogen optimisation through a grid-connected electrolyser: the case of GreenLab skive, Renew. Sust. Energ. Rev. 171 (113033) (2023).

[24] W. Dong, Z. Lu, L. He, J. Zhang, T. Ma, X. Cao, Optimal expansion planning model for integrated energy system considering integrated demand response and bidirectional energy exchange, CSEE J. Power Energy Syst. 9 (4) (2023).

[25] Y. Luo, X. Zhang, D. Yang, Q. Sun, Emission trading based optimal scheduling strategy of energy hub with energy storage and integrated electric vehicles, J. Mod. Power Syst. Clean Energy 8 (2) (2020).

[26] C. Li, N. Wang, Z. Wang, X. Dou, Y. Zhang, Z. Yang, F. Maréchal, L. Wang, Y. Yang, Energy hub-based optimal planning framework for user-level integrated energy systems: considering synergistic effects under multiple uncertainties, Appl. Energy 307 (118099) (2022).

[27] X. Luo, Y. Liu, J. Liu, X. Liu, Energy scheduling for a three-level integrated energy system based on energy hub models: a hierarchical Stackelberg game approach author links open overlay panel, Sustain. Cities Soc. 52 (101814) (2020).

[28] S. Cheng, R. Wang, J. Xu, Z. Wei, Multi-time scale coordinated optimization of an energy hub in the integrated energy system with multi-type energy storage systems, Sustain. Energy Technol. Assess 47 (101327) (2021).

[29] Z. Liu, M. Zeng, H. Zhou, J. Gao, A planning method of regional integrated energy system based on the energy hub zoning model, IEEE Access 9 (2021) 32161–32170.

[30] H. Chamandoust, G. Derakhshan, S.M. Hakimi, S. Bahramara, Multi-objectives optimal scheduling in SmartEnergy hub system with electrical and thermalresponsive loads, Environ. Climate Technol. 24 (1) (2020) 209–232.

[31] P. Miao, Z. Yue, T. Niu, A. Alizadeh, K. Jermsittiparsert, Optimal emission management of photovoltaic and wind generation based energy hub system using compromise programming, J. Clean. Prod. 281 (124333) (2021).

[32] Y. Qiao, F. Hu, W. Xiong, Z. Guo, X. Zhou, Y. Li, Multi-objective optimization of integrated energy system considering installation configuration, Energy 263 (125785) (2023).

[33] K. Zhang, B. Zhou, C.Y. Chung, S. Bu, Q. Wang, N. Voropai, A coordinated multi-energy trading framework for strategic hydrogen provider in electricity and hydrogen markets, IEEE Trans. Smart Grid 14 (2023) 1403–1417.

[34] C. Orozco, A. Borghetti, B.D. Schutter, F. Napolitano, G. Pulazza, F. Tossani, Intra-day scheduling of a local energy community coordinated with day-ahead multistage decisions, Sustain. Energy Grids Netw. 29 (100573) (2022).

[35] X. Zhang, X. Yu, X. Ye, S. Pirouzi, Economic energy managementof networked flexi-renewable energy hubs according to uncertainty modeling by the unscented transformation method, Energy 278 (128054) (2023).

[36] M. Tostado-Véliz, A.R. Jordehi, D. Icaza, S.A. Mansouri, F. Jurado, Optimal participation of prosumers in energy communities through a novel stochastic-robust day-ahead scheduling model, Int. J. Electr. Power Energy Syst. 147 (108854) (2023).

[37] M. Norouzi, J. Aghaei, S. Pirouzi, T. Niknam, M. Fotuhi-Firuzabad, Flexibility pricing of integrated unit of electric spring and EVs parking in microgrids, Energy 239 (122080) (2022).

[38] A. Najafi, O. Homaee, M. Jasiński, M. Pourakbari-Kasmaei, M. Lehtonen, Z. Leonowicz, Participation of hydrogen-rich energy hubs in day-ahead and regulation markets: a hybrid stochastic-robust model author links open overlay panel, Appl. Energy 339 (120976) (2023).

[39] M. Norouzi, J. Aghaei, T. Niknam, S. Pirouzi, M. Lehtonen, Bi-level fuzzy stochastic-robust model for flexibility valorizing of renewable networked microgrids, Sustain. Energy Grids Netw. 31 (100684) (2022).

[40] S. Pirouzi, Network-constrained unit commitment-based virtual power plant model in the day-ahead market according to energy management strategy, IET Gener. Transm. Distrib. 17 (22) (2023) 4958–4974.

[41] M. Tostado-Véliz, S.A. Mansouri, A. Rezaee-Jordehi, D. Icaza-Alvarez, F. Jurado, Information Gap Decision Theory-based day-ahead scheduling of energy communities with collective hydrogen chain, Int. J. Hydrog. Energy 48 (20) (2023) 7154–7169.

[42] A.R. Jordehi, M.S. Javadi, M. Shafie-khah, J.P.S. Catalão, Information gap decision theory (IGDT)-based robust scheduling of combined cooling, heat and power energy hubs, Energy 231 (120918) (2021).

[43] S.M. Moghaddas-Tafreshi, M. Jafari, S. Mohseni, S. Kelly, Optimal operation of an energy hub considering the uncertainty associated with the power consumption of plug-in hybrid electric vehicles using information gap decision theory, Int. J. Electr. Power Energy Syst. 112 (2019) 92–108.

[44] M. Kafaei, D. Sedighizadeh, M. Sedighizadeh, A.S. Fini, An IGDT/scenario based stochastic model for an energy hub considering hydrogen energy and electric vehicles: a case study of Qeshm Island, Iran, Int. J. Electr. Power Energy Syst. 135 (107477) (2022).

[45] M. Nasir, A.R. Jordehi, M. Tostado-Véliz, V.S. Tabar, S.A. Mansouri, F. Jurado, Operation of energy hubs with storage systems, solar, wind and biomass units connected to demand response aggregators, Sustain. Cities Soc. 83 (103974) (2022).

[46] A. Mobasseri, M. Tostado-Véliz, A.A. Ghadimi, M.R. Miveh, F. Jurado, Multi-energy microgrid optimal operation with integrated power to gas technology considering uncertainties, J. Clean. Prod. 333 (130174) (2022).

[47] L. Wang, H. Dong, J. Lin, M. Zeng, Multi-objective optimal scheduling model with IGDT method of integrated energy system considering ladder-type carbon trading mechanism, Int. J. Electr. Power Energy Syst. 143 (108386) (2022).

[48] C. Peng, Z. Xiong, Y. Zhang, C. Zheng, Multi-objective robust optimization allocation for energy storage using a novel confidence gap decision method, Int. J. Electr. Power Energy Syst. 138 (107902) (2022).

[49] A. Mansour-Saatloo, R. Ebadi, M.A. Mirzaei, K. Zare, B. Mohammadi-Ivatloo, M. Marzband, A. Anvari-Moghaddam, Multi-objective IGDT-based scheduling of low-carbon multi-energy microgrids integrated with hydrogen refueling stations and electric vehicle parking lots, Sustain. Cities Soc. 103197 (2021).

[50] M.R. Jokar, S. Shahmoradi, A.H. Mohammed, L.K. Foong, N.L. Binh, S. Pirouzi, Stationary and mobile storages-based renewable off-grid system planning considering storage degradation cost based on information-gap decision theory optimization, J. Energy Storage 58 (106389) (2023).

[51] W. Liu, C. Liu, P. Gogoi, Y. Deng, Overview of biomass conversion to electricity and hydrogen and recent developments in low-temperature electrochemical approaches, Engineering 6 (2020) 1351–1363.

[52] T.H.B. Huy, H.T. Dinh, D. Kim, Multi-objective framework for a home energy management system with the integration of solar energy and an electric vehicle using an augmented ε-constraint method and lexicographic optimization, Sustain. Cities Soc. 88 (104289) (2023).

[53] T.H.B. Huy, H.T. Dinh, D.N. Vo, D. Kim, Real-time energy scheduling for home energy management systems with an energy storage system and electric vehicle based on a supervised-learning-based strategy, Energy Convers. Manag. 192 (117340) (2023).

[54] Z. Ullah, S. Wang, J. Radosavljević, J. Lai, A solution to the optimal power flow problem considering WT and PV generation, IEEE Access 7 (2019).

[55] V.V.S.N. Murty, A. Kumar, Multi-objective energy management in microgrids with hybrid energy sources and battery energy storage systems, Prot. Control Mod. Power Syst. 5 (2) (2020).

[56] Y. Wang, Y. Qin, Z. Ma, Y. Wang, Y. Li, Operation optimisation of integrated energy systems based on cooperative game with hydrogen energy storage systems, Int. J. Hydrog. Energy 48 (95) (2023) 37335–37354.

[57] M.H. Rasool, O. Taylan, U. Perwez, C. Batunlu, Comparative assessment of multi-objective optimization of hybrid energy storage system considering grid balancing, Renew. Energy 216 (119107) (2023).

[58] Z. Yahia, A. Pradhan, Multi-objective optimization of household appliance scheduling problem considering consumer preference and peak load reduction, Sustain. Cities Soc. 55 (102058) (2020).

[59] M. Tostado-Véliz, S. Gurung, F. Jurado, Efficient solution of many-objective home energy management systems, Int. J. Electr. Power Energy Syst. 136 (107666) (2022).

[60] B. Mohammadi-ivatloo, M. Nazari-Heris, Robust Optimal Planning and Operation of Electrical Energy Systems, Springer Nature Switzerland AG, 2019.

[61] A. Soroudi, Power System Optimization Modeling in GAMS, Springer Nature, 2017.

[62] SG H2 Energy [Online]. Available, https://www.sgh2energy.com/economics, 2023.

[63] K. Kuan, B. Zhou, S.W. Or, C. Li, C.Y. Chung, N. Voropai, Optimal coordinated control of multi-renewable-to-hydrogen production system for hydrogen fueling stations, IEEE Trans. Ind. Appl. 58 (2) (2022).

[64] Red Electrica [Online]. Available, https://demanda.ree.es.

[65] M. Binder, M. Kraussler, M. Kuba, M. Luisser, Hydrogen From Biomass Gasification, IEA Bioenergy, 2019.

[66] "GAMS," GAMS Software GmbH, [Online]. Available: https://www.gams.com/latest/gamslib_ml/libhtml/gamslib_epscm.html.